

SP2 Report
On
Part 3: Characteristics of Polymeric Coatings

Author: Marjorie Valix

Chief Investigator: Marjorie Valix

Table of Contents

1.0 INTRODUCTION	4
1.1 STRUCTURE AND MORPHOLOGY.....	4
1.2 FILLER CHARACTERISTICS	6
1.2.2 <i>Filler Size</i>	6
1.2.1 <i>Elemental Composition of Fillers.</i>	7
1.3 EXTENT OF CURING AND HYDROPHOBICITY	8
1.3.1 <i>CNS Analysis.....</i>	8
1.3.2 <i>Extent of Curing</i>	9
1.3.3 <i>Hydrophobicity</i>	11
1.3.4 <i>Filler interaction with epoxy</i>	12
1.4 THERMAL DEGRADATION BEHAVIOR OF POLYMERIC COATINGS	14
1.5 BIODEGRABILITY OF POLYMERIC COATINGS	16
APPENDIX I. LIST OF POLYMERIC COATINGS.....	19
APPENDIX 2. SEM, EDS AND XRF ANALYSIS OF POLYMERIC COATINGS.....	20
2.0 SCANNING MICROSCOPY AND ELEMENTAL ANALYSIS OF EPOXY COATINGS.....	20
2.1 SUMMARY OF RESULTS	20
2.2 SIKADUR 41	22
2.3 SIKAGARD 63N	26
2.4 SIKAGARD 62T.....	29
2.5 FENCO S301 ULTRACOAT (UK).....	33
2.6 NITOMORTAR ELS (PHARCHEM)	37
APPENDIX 3 FOURIER TRANSFORM INFRARED SPECTROSCOPY (FTIR).....	42
3.0 FOURIER TRANSFORM INFRARED SPECTROSCOPY (FTIR).....	42
3.1 SUMMARY OF RESULTS	42
3.2 SIKADUR 41	44
3.3 SIKAGARD 63N AND SIKADUR 41	45
3.4 SIKAGARD 62T.....	46
3.5 FENCO S301	48
3.6 NITOMORTAR ELS	49
3.7 POLIBRID 705E.....	50
3.8 HYCHEM TL5.....	51
APPENDIX 4 THERMOGRAVIMETRIC ANALYSIS OF COATINGS	53
4.0 THERMOGRAVIMETRIC ANALYSIS OF COATINGS	53
4.1 SUMMARY OF RESULTS	53
4.2 SIKADUR 41	55
4.3 SIKADUR 63N AND SIKADUR 41	57
4.4 SIKAGARD 62T.....	58
4.5 FENCO S301	60
4.6 NITOMORTAR ELS	61
4.7 HYCHEM TL5.....	63
5.0 DIFFERENTIAL SCANNING CALORIMETRY (DSC)	64
5.1 FENCO S301	64

5.2 HYCHEM TL5.....	64
5.3 NITOMORTAR ELS	65
5.4 POLIBRID 705E.....	65
5.5 SIKADUR 31	66
5.6 SIKAGARD 63N	66
5.7 SIKADUR 41	67

1.0 Introduction

The polymeric coatings were characterised to examine both their physical and chemical features to relate these to their acid permeation properties. This was conducted as a basis for formulating specification of coating properties that would promote greater resistance to acid permeation and thus performance in the sewers. In this study, the following properties were considered:

- Structure/Morphology
- Filler characteristics

Percentage of filler used, chemical nature of the fillers, filler shape, size and distribution and chemical interaction of the filler with the epoxy.

- Extent of Curing
- Hydrophobicity (wetting properties)
- Thermal degradation properties of the coating
- Biodegradation properties

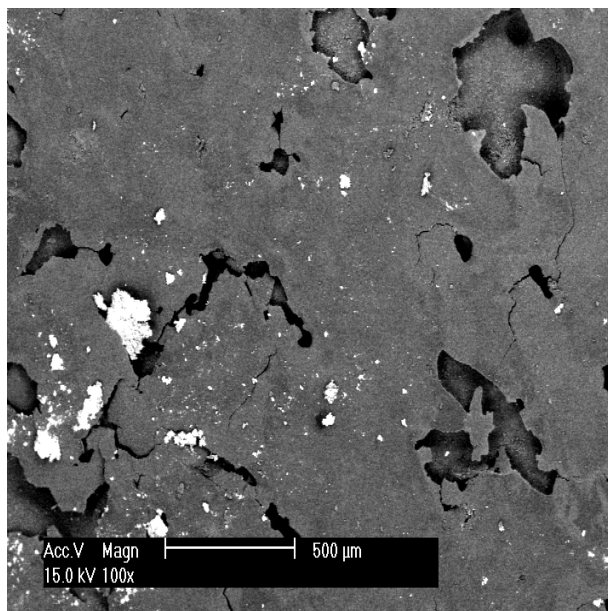
A summary of these properties are given below. The detailed characterisation of most of the polymeric coatings are shown in the Appendix section of this report.

1.1 Structure and Morphology

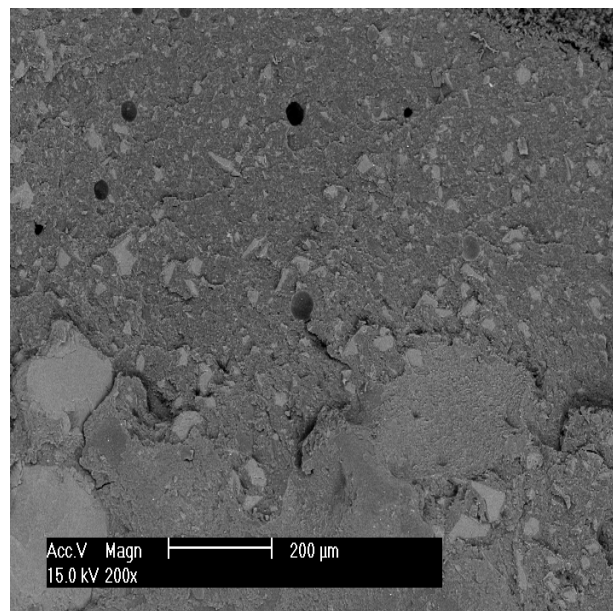
Even though polymeric coatings or mortar coatings are highly corrosion resistant, their performance is reduced by the presence of pinholes, pores and other defects. Pinholes are small holes that typically forms when bubbles within the coating ruptures. Pores that travel through the coating are particularly detrimental as they can result in premature failure of the coating. Other defects can include blisters, delamination and peeling.

The presence of pinholes was tested using a holiday test. All coupons were first tested to ensure they are free from pinholes before they were tested for degradation. The structural morphology of the coatings, filler size and distribution were examined using scanning electron microscopy. Energy Dispersive X-ray Spectroscopy or EDS analysis was used to provide a semi-quantitative analysis of the elemental components in the fillers.

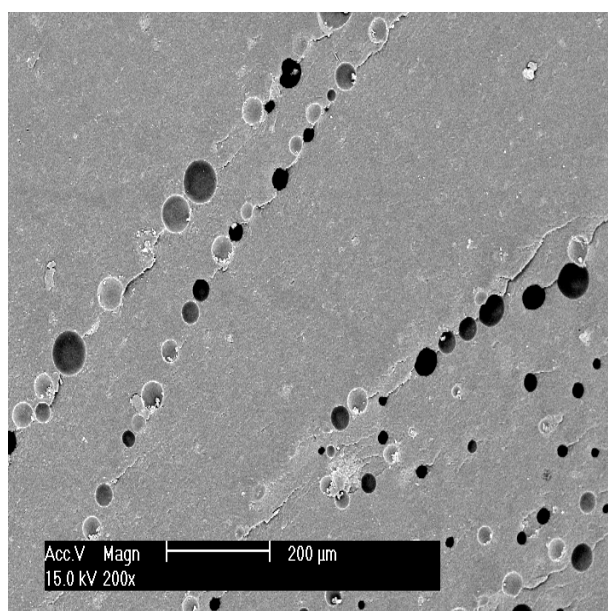
The morphology of four of the coatings assessed in this study are shown in Figure 1. Most of the coatings have small holes ($\sim 10\text{--}500\mu\text{m}$) on the surface. These appear to have been generated by air bubbles that have escaped during curing. The presence of the holes suggests that most of the coatings will only provide part of protection of its thickness.



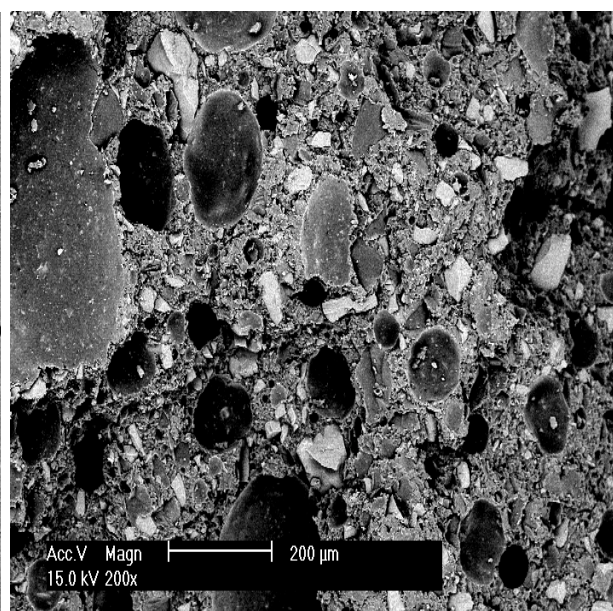
Sikadur 41



Sikagard 63N



Fernco S301



Nitomortar ELS

Figure 1. Scanning electron microscopy image of epoxy coatings.

1.2 Filler Characteristics

1.2.2 Filler Size

Most of the coatings have fillers. Being heavier in molecular weight, these shows up as bright spots in the SEM scan. Fillers do not appear to be present in Sikagard 63N and Fernco S301. In

Table 1. Summary of Coating Microanalysis by EDS and XRF.

NA (not available)

		Filler Characteristics		
Coating	Comments	Principle Filler	Shape	Size
Sikadur 41	Surface repair material	SiO ₂ (83%), CaO (2.9%)	Spherical	(< 50 – 250 µm)
Sikadur 31	Primer	SiO ₂ (67%), CaO (5.6%)	NA	NA
Sikagard 63 N		SiO ₂ (41.6%), TiO ₂ (2.9%), CaO (1%)	Spherical	(10 – 50 µm)
Nitomortar (Pharchem)		SiO ₂ (36%), MgO (1.6%)	Cubic & Spherical	100x50µm and <10 µm
Hychem TL5		SiO ₂ (20.2%), TiO ₂ (2.18%)	NA	NA
S301 (Fernco, UK)	Claimed 100% epoxy	SiO ₂ (7%), Al ₂ O ₃ (3%), TiO ₂ (1%)	Spherical	Not visible in SEM
Polibrid 705E	Claimed 100% polyurethane	SiO ₂ (0.69%), TiO ₂ (3.47%)	NA	NA

Sikadur 41, the fillers are unevenly distributed and a slightly spherical shape. Whereas in ELS, the shape of the filler are highly angular and with greater size distribution. A summary of the filler properties are given in Table 1.

1.2.1 Elemental Composition of Fillers

The elemental composition of the fillers present in the polymeric coatings were analysed by XRF. This analysis and the percentage fillers present in the coatings are reported in Table 2. As shown the coatings assessed in this study contained fillers from 5.7 to 87.8 wt%. Although the manufacturers claim that Fernco S301 and Polibrid contains 100% polymers, it is evident from the XRF analysis that these contain 13 and 5.7 wt% fillers respectively. The main components of the fillers is SiO_2 . Minor components include TiO_2 , this was perhaps used as colouring material, typically used as white pigment. The remaining heavy metal elements including Th, U and Zr suggest that mineral sand may have been used as the filler material.

Table 2. XRF analysis of the polymeric coatings.

Filler Components (%)	Sikadur 41	Sikadur 31	Sikagard 63N	Nitomortar ELS	Hychem TL5	Fernco S301	Polibrid 705E
Na_2O	0.21						
MgO	0.17			1.61			
Al_2O_3	0.48	0.17	0.52	0.31	0.09	3.08	0.5
SiO_2	83.09	67	41.59	36.56	20.2	6.98	0.69
P_2O_5	0.019						
SO_3	0.109		0.409	0.526		0.563	
K_2O	0.067	0.02	0.212	0.262	<0.01	0.326	0.14
ThO_2	0.015		0.076	0.085		0.127	
U_3O_8	0.008		0.022	0.024		0.032	
CaO	2.93	5.6	1.01	0.68	<0.01	0.79	<0.01
TiO_2	0.226	0.38	2.907	0.502	2.18	1.064	3.47
Cr_2O_3	0.095	0.1	0.172	0.109	0.03	0.107	<0.01
MnO	0.009	<0.01	0.018	0.015	<0.01	0.014	<0.01
Fe_2O_3	0.11	0.46	0.4	0.22	0.19	0.016	<0.01
NiO	0.237	0.227	0.416	0.131	0.074		<0.001
BaO	0.010						
CeO_2	0.013		0.108	0.159		0.243	
V_2O_5		<0.01	0.011	0.013		0.019	<0.01
ZrO_2		0.01	0.016			0.020	
PbO				0.011		0.017	
Total-Filler	87.8	73.967	47.9	41.32	22.76	13.0	5.7
LOI	12.86	26.34	54.01	59.24	77.17	88.04	94.3
Total	100.66	100.307	101.91	100.56	99.934	101.4	99.1

1.3 Extent of Curing and Hydrophobicity

1.3.1 CNS Analysis

The presence of sulfur and nitrogen in the coating has two important implications. The first is that sulfur and nitrogen are growth substrates for sulfur oxidizing and nitrifying bacteria. Their presence therefore could assist in supporting the growth of these organisms and thus the generation of biogenic acids. In addition amino group N-H and sulfate (SO_4^{2-}) and sulfonates (SO_3^{2-}) groups provide the epoxy with hydrophilic sites that promotes their absorption of water from their environment, thus reducing their effectiveness.

In addition amino groups (N-H) that have unpaired electrons provided epoxy with its hydrophilic properties ‘water-loving’. This promotes the adsorption of water from the environment which could result in a decrease in its protectiveness.

Loss on ignition (LOI) is representative of the component that volatilises at 1050°C and is considered to be representative of the organic component of the coatings.

The CNS and LOI for the various coatings considered in this study are shown in Table 3. Relative comparison of S and N contents of the coatings in Figure 2 show that Sikadur 41 has the least S and N content and may therefore be the least hydrophilic, whereas Fernco the most hydrophilic.

Table 3. LOI and CNS analysis of the polymeric coatings.

Components (%)	Sikadur 41	Sikadur 31	Sikagard 63N	Nitomortar ELS	Hychem TL5	Fernco S301	Polibrid 705E
LOI	12.86	26.34	54.01	59.24	77.17	88.04	94.3
Carbon	8.55		35.88	44.27		79.19	
Nitrogen	0.37		1.55	1.51		2.69	
Sulfur	0.109		0.409	0.526		0.563	

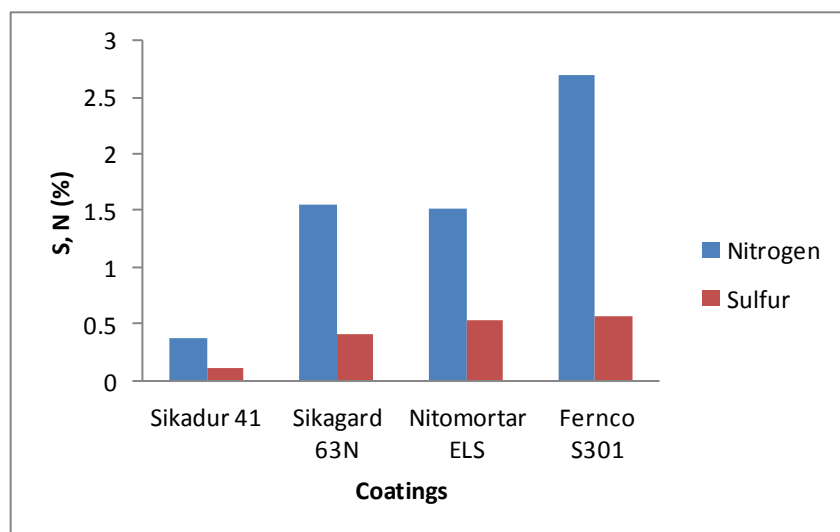


Figure 2. Sulfur and nitrogen contents of polymeric coatings

1.3.2 Extent of Curing

The curing reaction occurs in the process by the reaction of the end epoxy groups with the hardener. Epoxy rings open out and molecules become linked in a three-dimensional network. The decrease of end epoxy rings during the reaction can be measured by quantitative analysis using FTIR spectroscopy.

As an example, the FTIR spectroscopy spectrum of Sikadur 31 as shown in Figure 3, shows the bands of interest at $1606, 871$ and 3359 cm^{-1} .

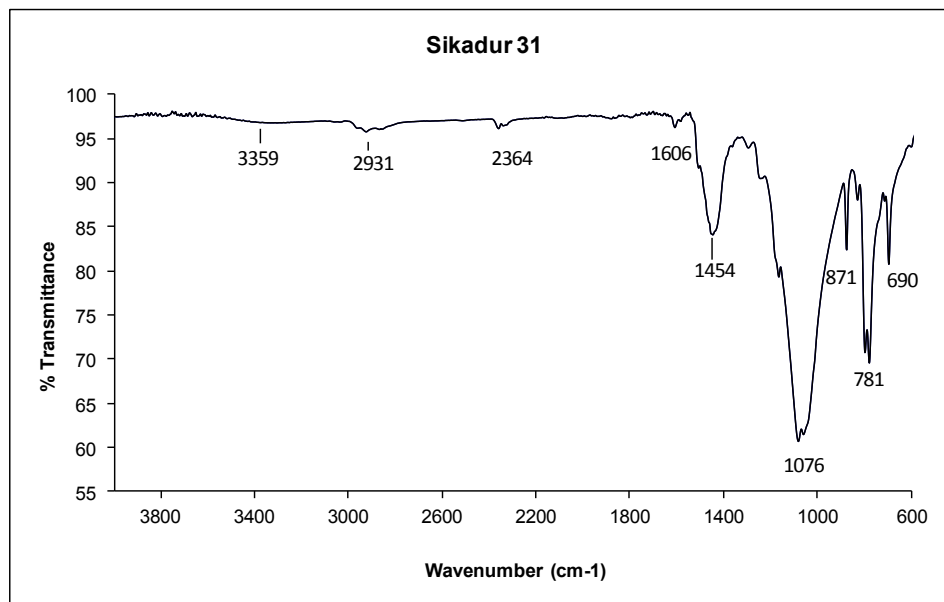


Figure 3. FTIR spectrum of the raw Sikadur 31 coating

The degree of curing is inversely proportional to the presence of epoxy resins. The relative degree of curing (R_c) was estimated using the following correlation:

$$R_c = \frac{A_{863/917}}{A_{1508/1610}} \quad (1)$$

Where $A_{863/917}$ and $A_{1508/1610}$ are the areas of the bands at these wavelength. The bands at 1610 cm^{-1} and 1508 cm^{-1} were used as quantitative reference. These are associated with the benzene ring present in the molecule of glycidic polyether. Absorbance of these bands do not vary during the curing reaction.

The intensity of the bands at 863 cm^{-1} and 917 cm^{-1} decreases during the curing reaction due to the opening of the epoxy rings. These were used as indicative bands for the progress of the reaction. The relative curing of the coatings are compared in Figure 4. Most of the coatings showed reasonable curing. It appears however that Sikadur 41 offered the highest curing.

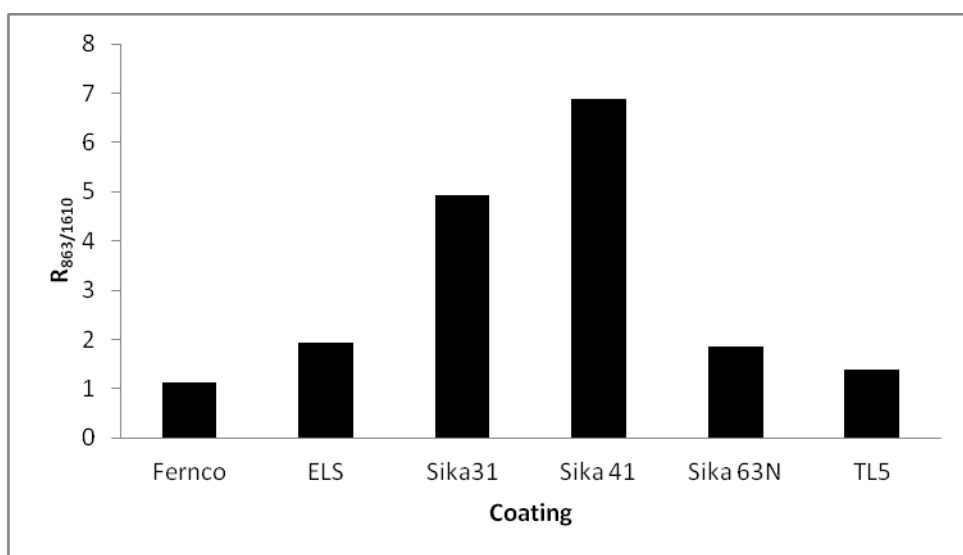


Figure 4. Relative curing of the epoxy coatings

The analysis above did not include Polibrid 705E, which is a polyurethane. The polyurethane reaction starts with a diisocyanate(or a poly-isocyanate) reacting with a comonomer like an alcohol (frequently a diol):



The FTIR spectra of Polibrid in Figure 5 shows the definite major polyurethane peaks at 3328 cm^{-1} associated with hydrogen bonded NH groups with urethane carbonyl group. Other major peaks identified from Polibrid as listed in Table 4 include the urethane carbonyl group in 1730 and 1706 cm^{-1} and NH deformation in 1523 cm^{-1} . The band in 1730 cm^{-1} is non-bonded urethane C=O stretching and the 1706 cm^{-1} is the bonded urethane C=O stretching, These

bands and the lack of OH band at 3350 cm⁻¹ confirms the formation of urethane linkages and the curing of this coating.

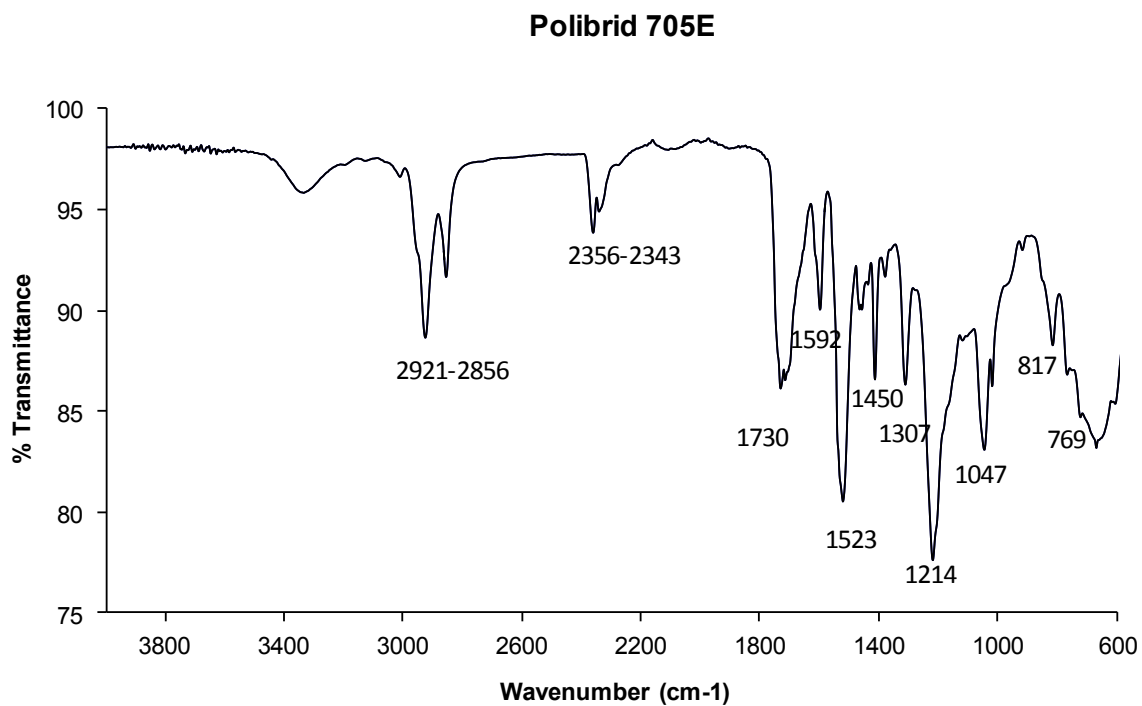


Figure 5. FTIR spectrum of the raw Polibrid 705E coating.

Table 4. Absorption band analysis in the IR analysis of Polibrid 705E.

Wavenumber (cm ⁻¹)	Assignments	Normalised %Height
3328	N-H stretching	18.7
2921-2856	Asymmetric stretching CH ₃ groups in -Si(CH ₃) ₂	50.8
2356 - 2343	CH ₂ and CH ₃ stretch methylene	26.9
1730	C=O, amine stretching , non-bonded urethane stretching	62.7
1523	NH, amide deformation	86.2
1450	CH ₂ , scissor	41.5
1307	OCOCH, wagging	61
1214		100
1047	OCONH, in plane vibrations	75.5
817	CH ₂ pendulum swing	51.9

1.3.3 Hydroproicity

FTIR also provides surface functional group analysis that reflect the surface chemistry of the epoxy. For example hydroxyl group (-OH), carboxyl group (C=O), sulphate and sulfonate groups (S=O) and amino group (N-H) have unpaired electron, polar and are therefore able to exhibit hydrophilic properties that attract water from the environment(Lemke 2012). This is an important feature because the higher uptake of moisture will reduce the effectiveness of

the coating in acting a barrier to corrosive environments. The band at 3390 cm^{-1} is indicative of OH group. The relative hydrophilic properties of the coatings were compared using the following ratio:

$$H = \frac{A_{3390}}{A_{1610}} \quad (3)$$

The relative hydrophilic properties of the coatings are compared in Figure 64. As shown most of the coating exhibited similar hydrophilic behaviour. The exceptions are Fernco S301 and Hychem TL5, which showed the almost half the hydrophilicity of the other epoxy coatings.

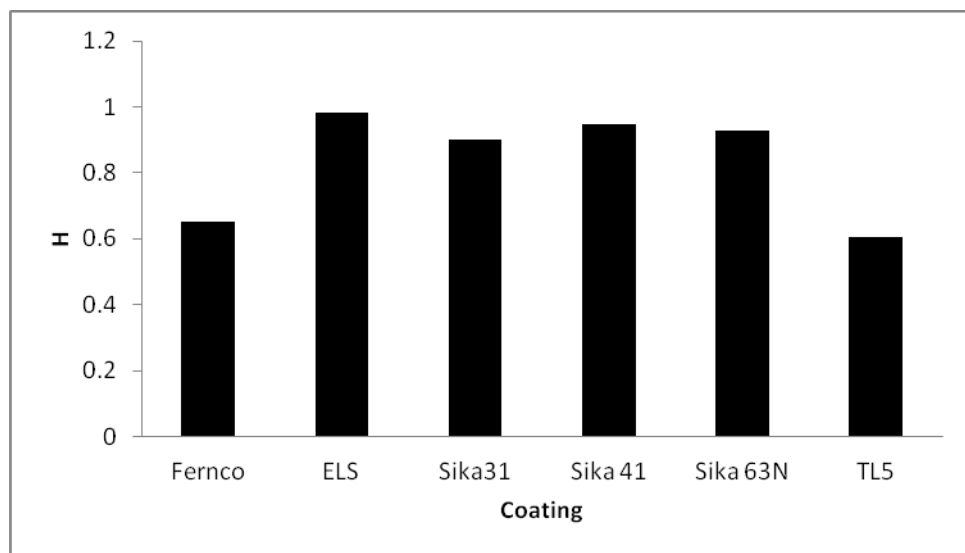


Figure 6. Hydrophilicity of epoxy coatings.

1.3.4 Filler interaction with epoxy

This suggests the filler in this epoxy material are present primarily as free fillers and only a relatively lower proportion of the filler has reacted with the epoxy

FTIR revealed that silica is present both as an oxide Si-O-Si and Si-C. The first reflect the free filler and the later reflects the interaction of the silica filler with the epoxy. This interaction has been suggested to provide the coating with better resistance to acid and water transport. The ratio between SiC to Si-O-Si provides the relative ratio of filler interaction with epoxy to the free filler. The FTIR band at $800\text{-}850\text{ cm}^{-1}$ is attributed to Si-C and $1082\text{-}1012\text{ cm}^{-1}$ to Si-O-Si. A summary the bands identified in the various coatings are given in Table 5 with the ratio of SiC to Si-O-Si. It appears ELS has the least ratio with 0.62 and Fernco S301 having the highest ratio of 1.30. The ranking of the coatings in terms of filter-epoxy interaction is : Fernco S301>Sikadur 41 and Sikadur 63N>Nitomortar.

Table 5. Summary of FTIR Analysis of Epoxy Coatings

Note: Polibrid was not included in this summary because it is a polyurethane (see Table 4 for Polibrid FTIR analysis)

Wavenumber (cm ⁻¹)	Vibrations	Sikadur 41	Sikadur 31	Sikagard 63N	Nitomortar ELS	Hychem LT5	Fernco S301
% Normalised Relative Heights							
3390	O-H stretch	8.2	19.9	9.6	18.36	9.6	
2956	Asymmetric stretching CH ₃ groups in Si(CH ₃) ₂ –	10.8			27	17	
2919-2887	C-H stretch methylene			24.9	19.8		18.4
2364 - 2353	S-H stretching	4.5	8.5	23.7	7.9	28.2	14.2
2019	Si-H stretch	3.5					
1608 -1508	C=O-O carboxylate ion, aromatic band stretching	0.7	9.4	21	11.6	30.2, 66.1	26
1570	Ba-C			36.8			
1246 and 1463	CH ₃ symmetric deformation of Si-CH ₃	17.3	39.7	36.1, 61.4	56.8	81.3	75.7
1188	stretching of SO ₂	54.6					
1091	C-O-Ba						
1168, 1089	C=S and C=O	99					
1060-1039	Si-O-Si stretching vibration	100	100	100	100	100	76.8
980	Ti-C						
950	Al-O						34.2
875	Si-OH	37.6	44.7				
830 and 657	TiO ₂						
827	Si-C stretching and rocking	86	78	72.5	62.1	81.7	100
732 and 636	C-H out of plane bending for aromatics	56	79.3	73	68	70.7	45.6
Ratio of Metal-C/Metal Oxide (main filler)	SiC/Si-O-Si	0.86	0.78	0.725	0.621	0.817	1.30

1.4 Thermal degradation behavior of polymeric coatings

The thermal properties of the polymeric coatings were examined using thermal gravimetric analysis and by DSC to establish their glass transition temperatures.

TGA measures the amount and rate (velocity) of change in the mass of a sample as a function of temperature or time in a controlled atmosphere. In these tests, the samples were heated with a ramp rate of 20°C/min to temperature up to 1000°C under nitrogen environment. The measurements are used primarily to determine the thermal and/or oxidative stabilities of materials as well as their compositional properties. The technique was used to analyse material composition exhibited either through mass loss or gain due to decomposition, oxidation or loss of volatiles (such as moisture).

Figure 6 shows the TGA results for Sikadur 41. The TGA result shows Sikadur 41 underwent degradation at three temperatures, 105, 360 and 715°C. The low temperature endothermic peak is most likely to be associated with loss of water and any solvent residue. The Td at 360°C is attributed to the decomposition of silicate filler-epoxy polymer network and the higher Td (715°C) to the dehydrolylation of the filler. Gizdavic-Nikolaidis et al (Gizdavic-Nikolaidis et al. 2008) has shown the decomposition to SiO₂ occurs at about 700°C, which is consistent with our observation in Figure 7. The corresponding weight losses and assignments associated with each thermal decomposition temperatures are summarised in Table 7.

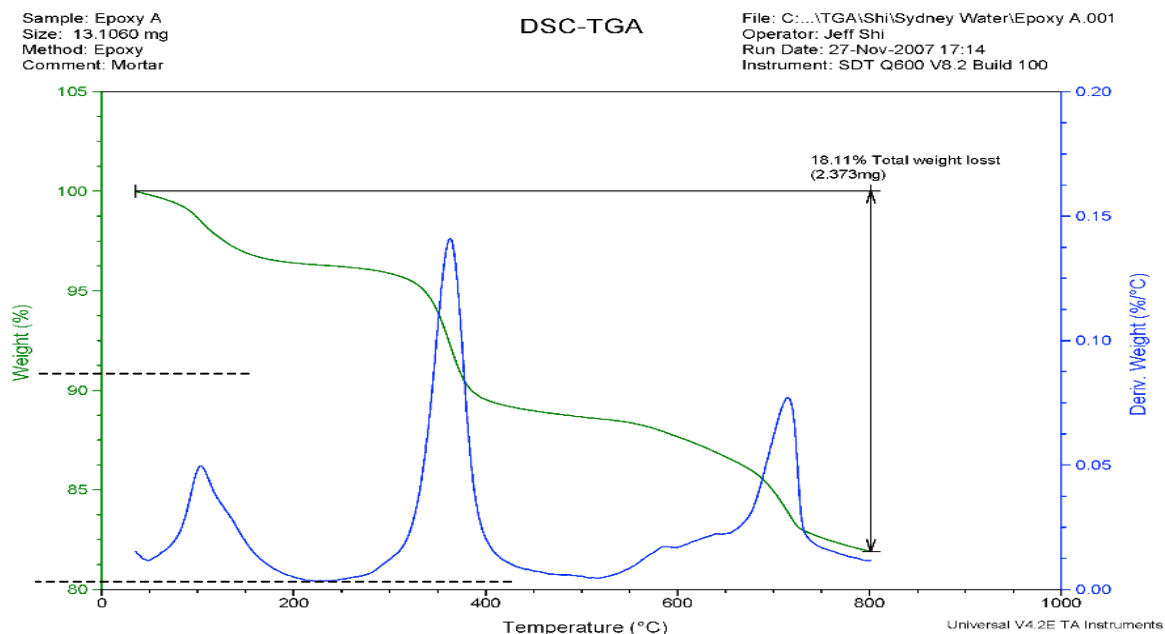


Figure 7. TGA thermogram of Sikadur 41.

Table 7. Thermal decomposition regions in Sikadur 41.

Optimum Degradation Temperature (°C)	Weight Loss (wt%)	Attributed Weight Loss
105	3.75	Moisture
360	7.5	Epoxy-Silicate
715	6.86	Dehydroxylation of the SiO ₂ H ₂ O

A summary of the thermogravimetric analysis of the coatings used in this study are shown in Table 8.

Table 8. Thermal decomposition temperatures of coatings

Assignment of weight loss (%)	Pure Epoxy	Thermal degradation temperature (°C)							
		Sikadur 41	Sikadur 31	Sikagard 63	Nitomortar ELS	Hychem TL5	Fernco S301	Polibrid	
Moisture + uncured resin		98-105		105	138	165	165		
Filler-Epoxy	350	343-360	343-360	350-360	370	369.2	378.5		
Dehydroxylation of Filler		715		675,715					
Weight Loss (wt%)									
Filler-Epoxy		7.5		41.2	50	54.5	73.28		

It has been shown that the filler can affect the the degradation of epoxy. The grafting of the filler with the resin will restrict the movement of polymer and the degradation of the polymers will shift to higher temperatures (Borchert et al. 2007, Chandradass and Bae 2008, Gisdavic-Nikolaidis et al. 2008, Hong et al. 2007, Ohman and Persson 2007, Tsai et al. 2008, Yan et al. 2008). The typical degradation of neat epoxy is around 350 °C and as shown in Table 8, the degradation temperatures of the epoxy with filler increased. The weight loss around 350-380 °C provides an indication of the extent of crosslinking between the filler and epoxy. Among the coatings tested Fernco S301 provided the highest temperature of degradation and the highest quantity of crosslinked epoxy-filler followed by Hychem TL5,

Nitomortar ELS and Sikagard 63N. Sikadur 41 providing also some crosslinking with the filler but at the lower temperature and lower concentration of filler-epoxy groups.

The glass transition temperatures of the polymeric coatings are reported in Table 9.

Table 9. The glass transition temperatures of the polymeric coatings

Glass transition temperature (°C)					
Sikadur 41	Sikagard 63	Nitomortar ELS	Hychem TL5	Fernco S301	Polibrid
71.13	104.3	76.57	101.51	69.29	77.77

1.5 Biodegradability of Polymeric Coatings

The following was used to establish the ability of the epoxy coating to support the growth of fungi using ASTM G21-96 (2002): Standard Practice for Determining Resistance of Synthetic Polymeric Materials to Fungi. Photographs of various epoxy coatings at day 0 of the test and after 28 days after inoculation with fungi are shown in Figure 66.

In these tests no other growth substrate were supplied to the organism as such any growth can only be supported if the organism is able to consume components of the coating. The samples were maintained in 95% humidity environment at about 28 °C and were examined for 28 days.

Growth were characterised as follow:

- 0, no growth;
- 1, traces of growth (less than 10% coverage);
- 2, light growth (10 to 30%);
- 3, medium growth (30 to 60%) and
- 4, heavy growth (60% to complete coverage).

A summary of the growth analysis is shown in Table 10. Within 28 days, there is very little growth of fungi on the coating materials. These results reveal that by these tests, the coatings are resistant to fungi growth. Examination, however of the coupons that have been installed in the sewer reveal than within 6 months, there is significant reduction in the surface pH revealing the proliferation, growth and metabolism of acid on the coating surface. This suggests that perhaps the standard testing should be extended to longer periods. However such testing should if at all possible reflect the various types of organisms present in the sewer.

Table 10. Fungi Growth Test on Polymeric Coatings

Coating	Time (days)								
	1	3	6	9	14	17	21	24	28
Sikadur 41	0	0	0	0	0	0	0	1	1
Fernco S301	0	0	0	0	0	0	1	1	1
Nitomortar ELS	0	0	0	0	0	0	0	0	0
Sikagard 63N	0	0	0	0	0	0	0	0	0

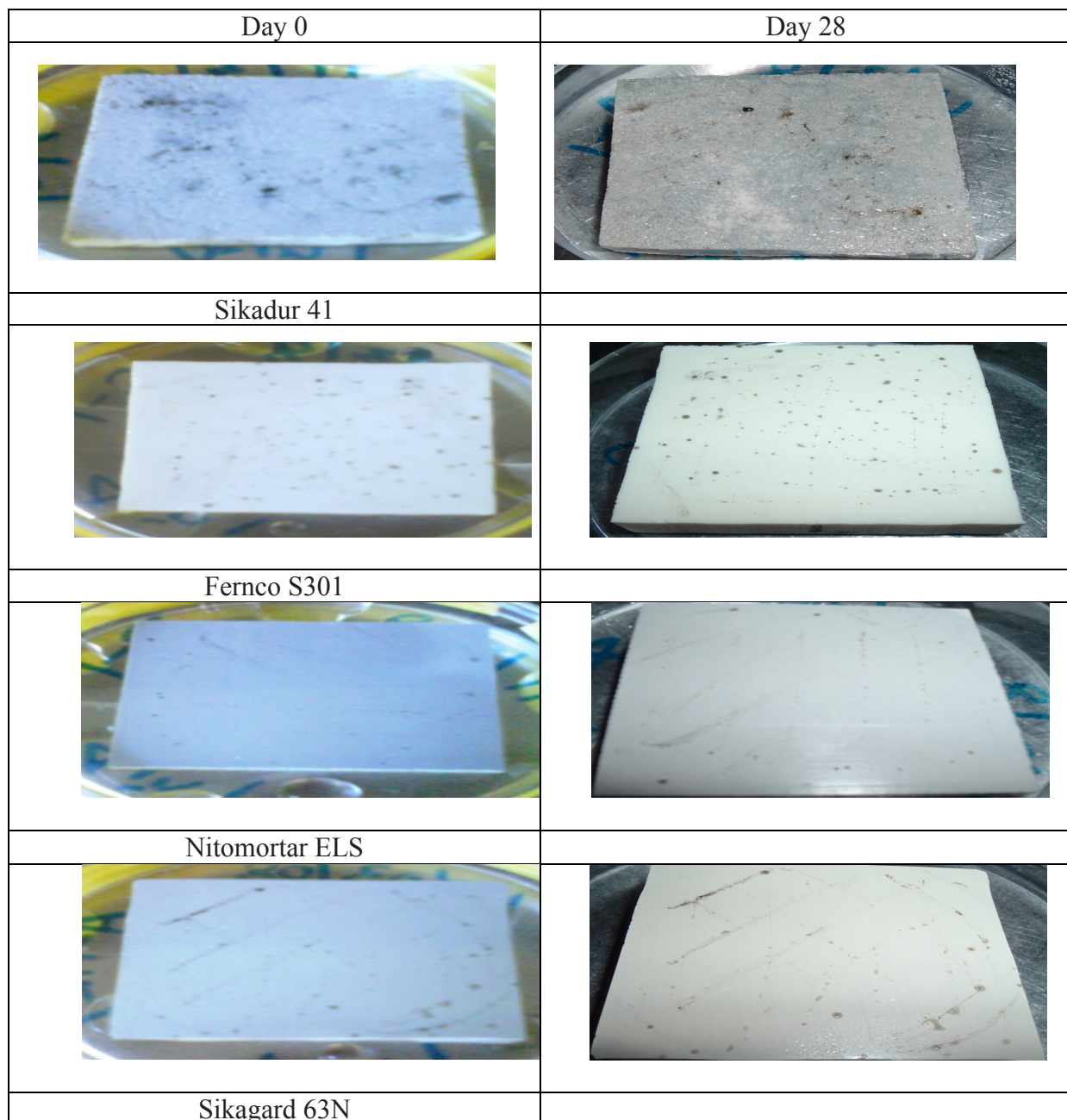


Figure 8. Photos of microbial growth test

References

- Borchert H, Jurgens B, Zielasek V, Rupprechter G, Giorgio S, Henry CR, Baumer M. 2007. Pd nanoparticles with highly defined structure on MgO as model catalysts: An FTIR study of the interaction with CO, O-2, and H-2 under ambient conditions. *Journal of Catalysis* 247: 145-154.
- Chandradass J, Bae DS. 2008. Preparation and properties of barium titanate nanopowder/epoxy composites. *Materials and Manufacturing Processes* 23: 117-123.
- Gizdavic-Nikolaidis MR, Edmonds NR, Bolt CJ, Easteal AJ. 2008. Structure and properties of GPTMS/DETA and GPTMS/EDA hybrid polymers. *Current Applied Physics* 8: 300-303.
- Hong RY, Fu HP, Zhang YJ, Liu L, Wang J, Li HZ, Zheng Y. 2007. Surface-modified silica nanoparticles for reinforcement of PMMA. *Journal of Applied Polymer Science* 105: 2176-2184.
- Lemke TL, Roche, V., and Zito, W. 2012. Review of Organic Functional Groups: Introduction to Medicinal Organic Chemistry Wolters Kluwer Lippincott Williams and Wilkins.
- Ohman M, Persson D. 2007. An integrated in situ ATR-FTIR and EIS set-up to study buried metal-polymer interfaces exposed to an electrolyte solution. *Electrochimica Acta* 52: 5159-5171.
- Simor M, Fiala A, Kovacik D, Hlidek P, Wypkema A, Kuipers R. 2007. Corrosion protection of a thin aluminium layer deposited on polyester. *Surface & Coatings Technology* 201: 7802-7812.
- Tsai TY, Lu ST, Huang CJ, Liu JX, Li CH, Chen LC, Ray U. 2008. The structure-property relationship of novolac cured epoxy resin/clay nanocomposites. *Polymer Engineering and Science* 48: 467-476.
- Yan H, Liao ZJ, Zhu X, Wang XM, Chen Y, Zhang B, Chen SL, Za ZY. 2008. Synthesis and electrorheological properties of polyaniline-coated barium titanate composite particles. *Journal of Applied Polymer Science* 107: 1960-1966.

Appendix I. List of Polymeric Coatings

Coating Name Plate	Type of Polymeric Materials (Manufacturer's TDS)	Advantages (Manufacturer's TDS)	Manufacturer	Website	Type of Polymer
Sikadur 41	This is 3-component thixotropic mortar based on a solvent free epoxy resin with aggregates	Chemical resistant	Sika Australia Pty Limited	www.sika.com.au	Epoxy A and F (mortar)
Sikadur 31	Thixotropic adhesive mortar based on a 2 component solvent free epoxy resin containing filler	Chemical resistant and insensitive to moisture during application, cure or whilst in service	Sika Australia Pty Limited	www.sika.com.au	Epoxy A (mortar)
Sikagard 63N	This is a two component solvent-free high build thixotropic protective coating based on epoxy resin.	Excellent chemical resistance	Sika Australia Pty Limited	www.sika.com.au	Epoxy F (100% epoxy)
Sikagard 62T	Two component high build thixotropic protective coating based on epoxy resin	Excellent chemical resistance	Sika Australia Pty Limited	www.sika.com.au	Epoxy A (mortar)
Nitomortar ELS	Nitomortar ELS is a solvent free, two component system consisting of epoxy resins and chemicals, incorporating a special blend of chemical resistant fillers.	Chemical and biologically resistant	Pharchem Construction Supplies	www.parchem.com.au	Epoxy A (mortar)
Hychem TL5	This is a two component solvent-free high thixotropic protective coating based on epoxy resin	Chemical resistant	Hychem International Pty Ltd.	www.hychem.com.au	Novolac (100% epoxy)
Polibrid 705E	This is a two component solvent free elastomeric urethane coating with geotextile fabrics (100% polypropylene) embedded within the coating to produce reinforced, bonded geomembrane linings	Chemical resistant	International Protective Coating (Akzo Nobel)	www.international-pc.com	Polyurea
Fernco Ultracoat S310	This is a two component solvent-free high build thixotropic protective coating based on epoxy resin.	Chemical resistant	Fernco Australia Pty Ltd	www.fernco.com.au	Epoxy

Appendix 2. SEM, EDS and XRF Analysis of Polymeric Coatings

2.0 Scanning Microscopy and Elemental Analysis of Epoxy Coatings

2.1 Summary of Results

This aspect of the study examined the properties of the epoxy coating fillers. Inorganic fillers have an important role in improving both the material properties (hardness and resilience) of coating and ability of coatings to reduce the transport of acids. The chemical nature of the fillers has an important impact on their reactivity towards acids and thus their life. The uses of oxides of specific metals lend such properties. In addition the particle size of the filler also has an important effect. It is widely accepted, for example that the inorganic fillers do not absorb moisture, thus their role in preventing moisture uptake into the coating is by providing a tortuous path for the moisture. Their roles in acidic environment are more complex, as acids can react with inorganic oxides. Thus the shape, size and distribution of the fillers, which all have impact on the acid path, can affect the life and effectiveness of epoxy coatings. The analysis of these factors was therefore considered in this study.

Sulfur and nitrogen are growth substrates for sulfur oxidizing and nitrifying bacteria. Their presence therefore could assist in supporting the growth of these organisms and thus the generation of biogenic acids. In addition amino group N-H and sulfate (SO_4^{2-}) and sulfonates (SO_3^{2-}) groups provide the epoxy with hydrophilic sites that promotes their absorption of water from their environment, thus reducing their effectiveness. As shown in Table AI, N is a component of epoxy matrix and therefore varies linearly with the loss of ignition (LOI%). LOI is the component that volatilizes from the coating under thermal treatment and reflects the polymeric composition of the coating.

A summary of the filler and S, N analyses of the coatings are shown below S301 appear to provide the best properties (Table AI). The particle size of its filler, although low in quantity, is very fine and was not detectable with SEM. In addition surface analysis suggests the coatings have little porosity again that could be detected by the SEM. It does have air bubble holes, which are present in all the coatings.

Table 2.1: Summary of Coating Microanalysis by EDS and XRF.

Coating	Filler Characteristics			LOI%	S (w/w)	N (w/w)%
	Principle Filler	Shape	Size		% (as SO ₃)	(w/w)%
Sikadur 41	SiO ₂ (83%), CaO (2.9%)	Spherical	(< 50 – 250 µm)	12.9	0.109	0.37
Sikagard 63 N	SiO ₂ (41.6%), TiO ₂ (2.9%), CaO (1%)	Spherical	(< 50 – 250 µm)	54	0.409	1.55
Sikagard 62T	BaO (17%), TiO ₂ (5.1%), SiO ₂ (2.37%), Al ₂ O ₃ (1%), CaO (1%),	Spherical	5-10 µm	69.5	4.05	1.73
S301 (Fernco, UK)	SiO ₂ (7%), Al ₂ O ₃ (3%), TiO ₂ (1%)	Spherical	Not visible in SEM	88	0.56	2.69
Nitomortar (Pharchem)	SiO ₂ (36%), MgO (1.6%)	Cubic & Spherical	100x50µm and <10 µm	59.2	0.53	1.51

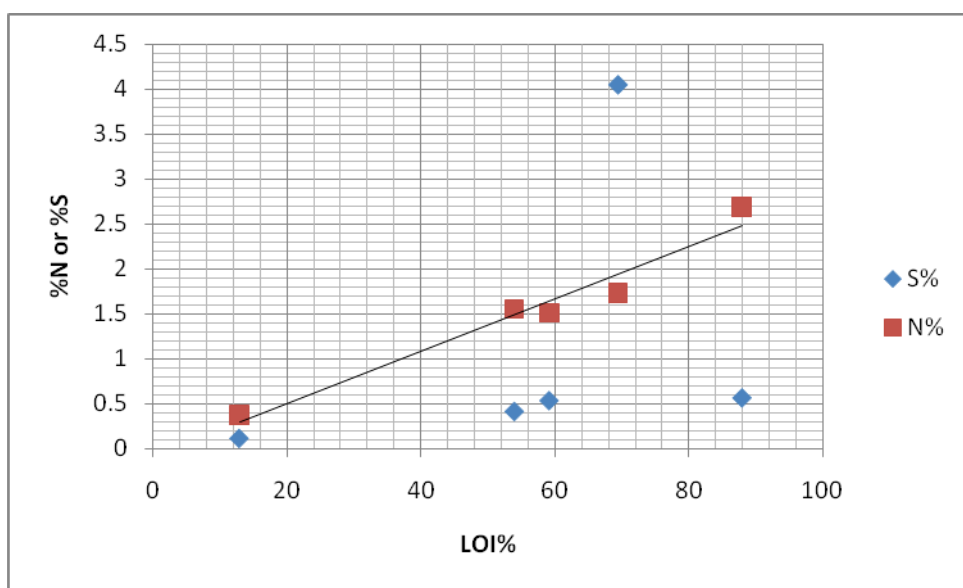


Figure 2.1: The correlations between S and N contents and LOI of epoxy coatings.

2.2 Sikadur 41

Scanning electron microscopy (SEM) examination of the backscattering image of Sikadur surface is shown in Figures 2.1 and 1.2. The cracks and holes are indicative of air bubbles within the epoxy during epoxy curing. The bright spots in the image reflect high molecular weight inorganic fillers. The filler are more obvious in Figure 2.1. As shown various sizes (< 50 – 250 μm) of fillers are visible. It is possible that there are smaller sized fillers; however the resolution of the SEM will not allow viewing of particles lower than 1 μm .

X-ray microanalysis of the epoxy surface was conducted using Energy Dispersive X-ray Spectroscopy or EDS analysis. The qualitative results are summarized in Table 2.1. As shown the main fillers are Si and Ca based inorganic compounds with minor quantities of Ag. EDS analysis of specific spots in Figure A 1.2, shows concentrations of Ag (Table 2.2) and Si and Ca (Table 2.3) in the fillers. EDS provides a rapid but qualitative elemental composition analysis with a sampling depth of 1-2 microns. A bulk analysis was therefore conducted by X-ray fluorescence on finely ground epoxy sample. The XRF results summarised in Table 2.4 confirms the presence of Si and Ca, although the Si composition suggested by this bulk analysis is higher (83%) in comparison to the 31% by the surface EDS analysis. The presence of minor quantities of TiO_2 , Fe_2O_3 , CeO_2 , ThO_2 , U_3O_8 , suggest the use of mineral sands in this epoxy. The loss of ignition (LOI) in Table 2.5 reflects that this coating is principally inorganic.

Sulfur and nitrogen based compound could become growth substrates that may support the growth of sulphur oxidising bacteria and nitrifying bacteria. In addition amino groups (N-H) that have unpaired electrons provided epoxy with its hydrophilic properties ‘water-loving’. This promotes the adsorption of water from the environment which could result in a decrease in its protectiveness. Both Tables 2.4 and 2.5 reflect the presence of minor quantities of S (0.1% in the form of SO_3) and N (0.37%) respectively.

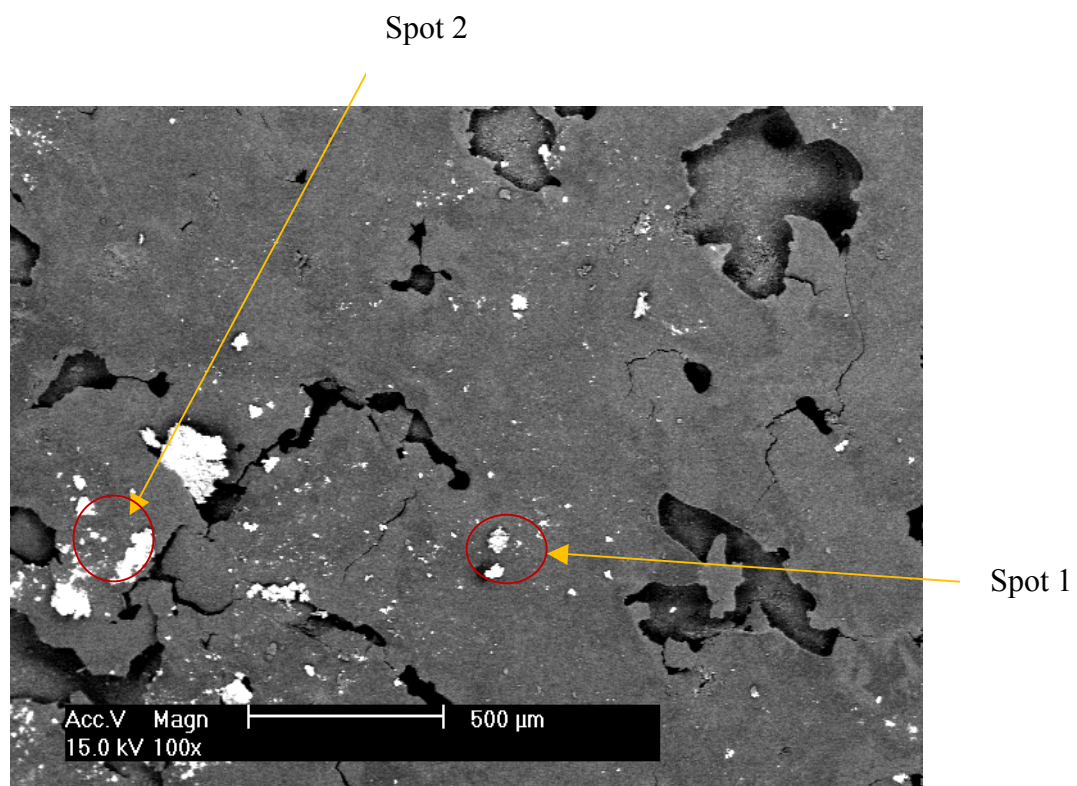


Figure 2.2: SEM image of Sikadur 41.

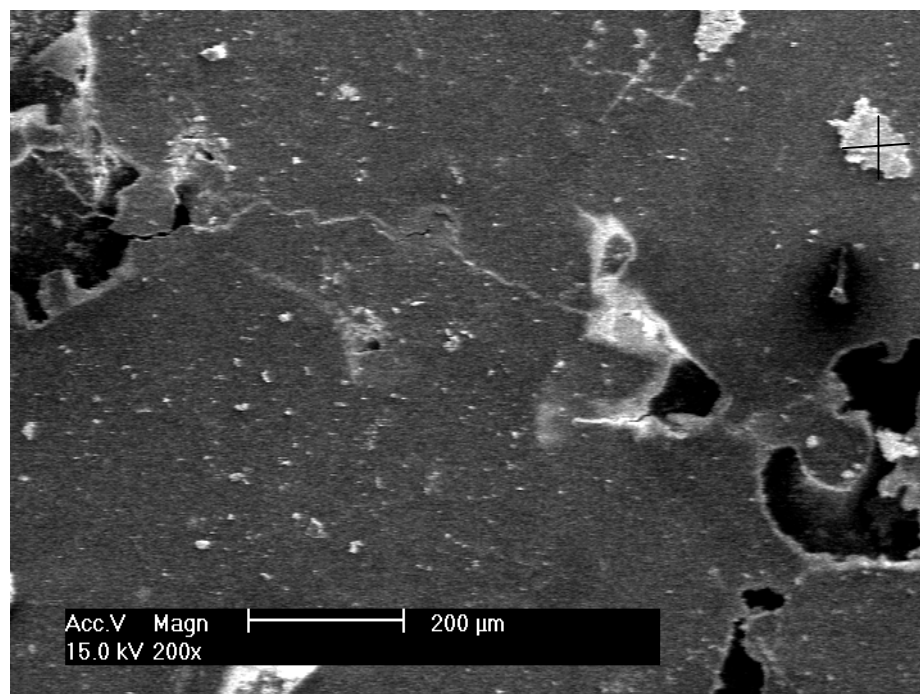


Figure 2.3: SEM image of Sikadur 41

Table 2.2: EDS average analysis of elemental composition of Sikadur 41.

Element	Wt %	At %	K-Ratio	Z	A	F
C	45.15	66.33	0.0826	1.0407	0.1758	1.0001
O	6.23	6.87	0.0093	1.021	0.1469	1.0002
Si	31.29	19.66	0.2737	0.9685	0.9015	1.002
Cl	0.99	0.5	0.0078	0.9167	0.8533	1.0078
Ag	1.96	0.32	0.0155	0.7651	1.0283	1.0106
Ca	14.38	6.33	0.1286	0.9391	0.9519	1
Total	100	100				

Table 2.3: EDS Spot 1 analysis of elemental composition of Sikadur 41.

Element	Wt %	At %	K-Ratio	Z	A	F
Si	30.26	39.16	0.2469	1.0361	0.7827	1.0061
Cl	3.43	3.51	0.028	0.9743	0.8186	1.0258
Ag	4.92	1.66	0.0407	0.8127	0.9841	1.0363
Ca	61.4	55.67	0.5615	0.9983	0.9161	1
Total	100	100				

Table 2.4: EDS Spot 2 analysis of elemental composition of Sikadur 41.

Element	Wt %	At %	K-Ratio	Z	A	F
Si	7.37	19.33	0.0537	1.224	0.5909	1.0083
Ag	77.56	52.96	0.7356	0.9421	1.0019	1.0049
Ca	15.08	27.71	0.1203	1.1605	0.6876	1
Total	100	100				

Table 2.5: XRF analysis of elemental composition of Sikadur 41.

Compound	Value	Unit	Compound	Value	Unit
Na ₂ O	0.21	%	BaO	0.010	%
MgO	0.17	%	CeO ₂	0.013	%
Al ₂ O ₃	0.48	%	ThO ₂	0.015	%
SiO₂	83.09	%	U ₃ O ₈	0.008	%
P ₂ O ₅	0.019	%			
SO ₃	0.109	%			
K ₂ O	0.067	%			
CaO	2.93	%			
TiO ₂	0.226	%			
Cr ₂ O ₃	0.095	%			
MnO	0.009	%			
Fe ₂ O ₃	0.11	%			
NiO	0.237	%			
Total	87.8	%			
Actual Total	100.66	%			

Table 2.6: C, N analysis of Sikadur 41.

Type:	Routine
Archive:	BEAD1
Application:	BEAD1
Init Weight:	0.84g
Flux Weight:	4.5g
Final Weight:	5.34g
LOI (%):	12.86
Carbon (%):	8.55
Nitrogen (%):	0.37

2.3 Sikagard 63N

SEM examination of Sikagard 63N (Figure 2.4) also shows the presence of holes from air bubbles. The filler size also appears to be in the regions of ($< 50 - 250 \mu\text{m}$). EDS analysis in Table A2.7, suggest the main fillers are Si and Ca and minor quantities of Ag. XRF analysis in Table A2.8, confirms the presence of Si and Ca, although again the bulk Si content (41.6%) is relatively higher in comparison to Ca. Minor quantities of TiO_2 , Fe_2O_3 , CeO_2 , ThO_2 , U_3O_8 reflect the use of mineral sands as filler in this coating. This coating appears similar to Sikadur 41 with the exception that its LOI (54%, Table 2.9) suggest a greater proportion of epoxy to filler. The coatings contain higher S (0.409% as SO_3) and N (1.55%). The later reflecting it's more hydrophilic property in comparison to Sikadur 41.

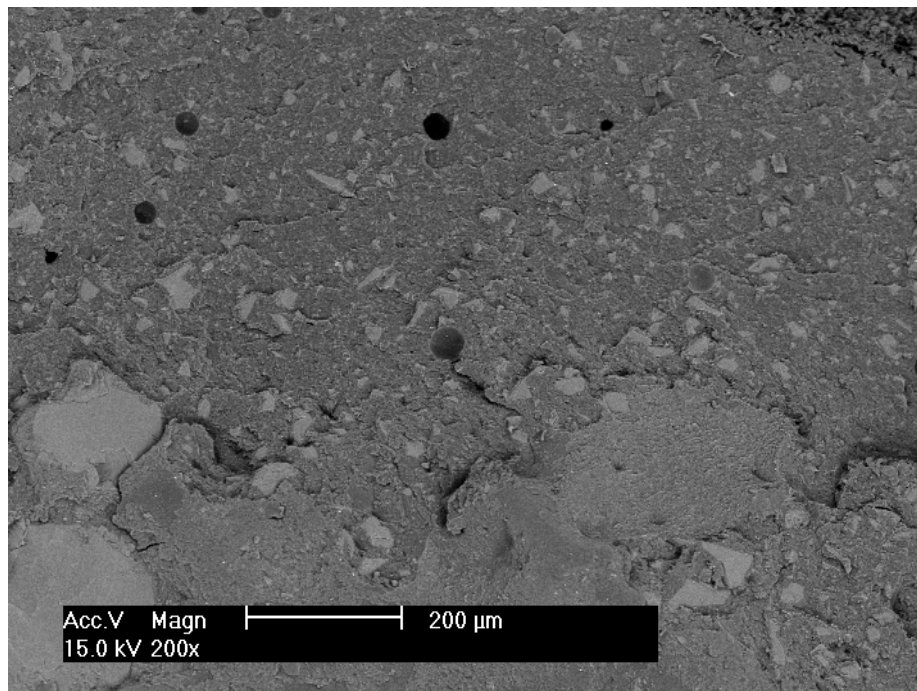


Figure 2.4: SEM image of Sikagard 63N.

Table 2.7: EDS average analysis of elemental composition of Sikagard 63N.

Element	Wt %	At %	K-Ratio	Z	A	F
C	42.91	67.17	0.1009	1.0481	0.2242	1.0002
O	3.48	4.09	0.0044	1.0281	0.1224	1.0002
Si	20.56	13.76	0.1738	0.977	0.8621	1.0038
Cl	1.02	0.54	0.0085	0.9238	0.8915	1.0172
Ag	1.97	0.34	0.0165	0.771	1.0616	1.0255
Ca	30.06	14.1	0.2756	0.9464	0.9688	1
Total	100	100				

Table 2.8: XRF analysis of elemental composition of Sikagard 63N.

Compound	Values	Unit
Al ₂ O ₃	0.52	%
SiO ₂	41.59	%
SO ₃	0.409	%
K ₂ O	0.212	%
CaO	1.01	%
TiO ₂	2.907	%
V ₂ O ₅	0.011	%
Cr ₂ O ₃	0.172	%
MnO	0.018	%
Fe ₂ O ₃	0.4	%
NiO	0.416	%
ZrO ₂	0.016	%
CeO ₂	0.108	%
ThO ₂	0.076	%
U ₃ O ₈	0.022	%
Total	47.9	%
Actual Total	101.91	%

Table 2.9: C and N analysis of Sikagard 63N.

Type:	Routine
Archive:	BEAD1
Application:	BEAD1
Init Weight:	0.84g
Flux Weight:	4.5g
Final Weight:	5.34g
LOI (%):	54.01
Carbon (%):	35.88
Nitrogen (%):	1.55

2.4 Sikagard 62T

SEM examination of Sikagard 62T (Figure 2.5) in 50 x magnification show relatively larger quantities of air bubble holes in comparison to Sikadur 41 and Sikagard 62T. Viewing this coating at 1000 x magnification in Figure 2.6 shows densely packed material covered with finer distribution of fillers. The fillers appear to be in the order of 5 – 10 µm but it appears the filler sizes are more uniformly distributed in comparison to Sikadur 41 and Sikagard 63N.

EDS analysis of two spots in the coating (Figure 2.6) suggest the fillers are Ba and Ti based with only minor Si. It is also surprising that this coating contains a huge proportion of S (11.27%) in the bright spot and 2% in the general lighter area.

XRF analysis (Table 2.10) confirms the presence and the relatively quantities of Ba and Ti. It also confirms the presence of higher quantity of S (4% in the form of SO₃).

The LOI in Table 2.11 of 69.5, reflect the relatively higher proportion of epoxy in this coating in comparison to Sikadur 41. This coating contains relatively higher S (2%) and N (1.73%) in comparison to Sikadur 41 and Sikagard 63N. The higher N reflecting its more hydrophilic nature.

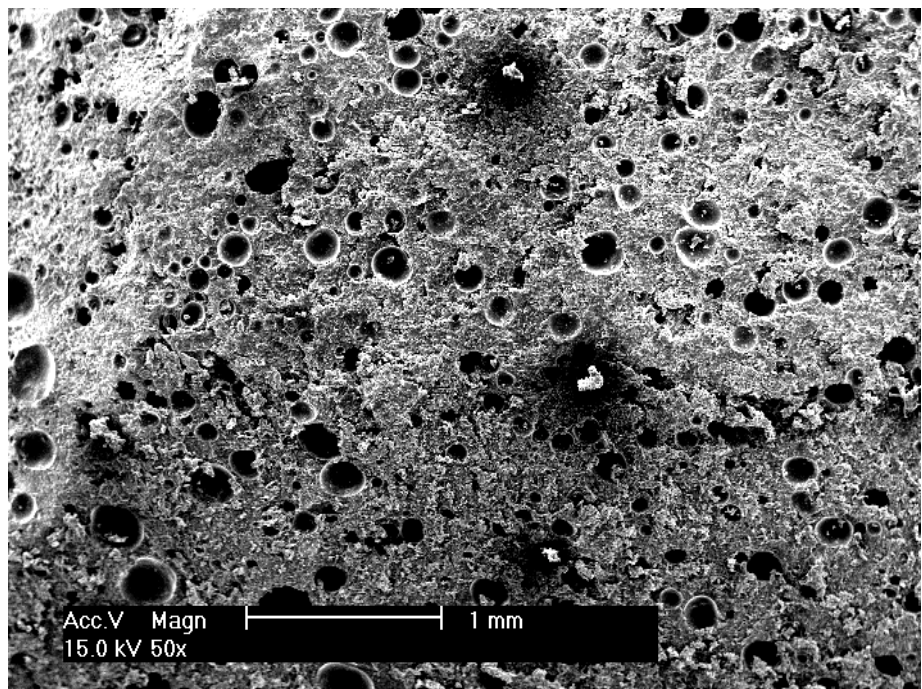


Figure 2.5: SEM image of Sikagard 62T.

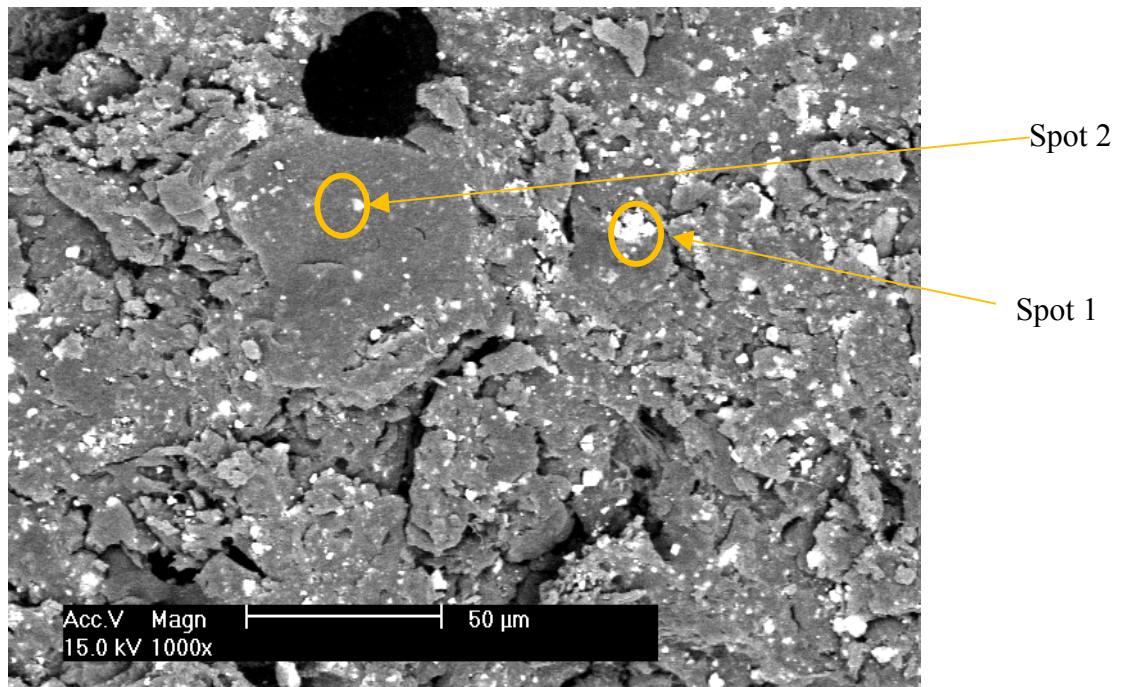


Figure 2.6: SEM image of Sikagard 62T.

Table 2.10: EDS spot 1 analysis of elemental composition of Sikagard 62T.

Element	Wt %	At %	K-Ratio	Z	A	F
C	14.63	54.48	0.0343	1.2657	0.1851	1
O	0.64	1.8	0.0019	1.2404	0.2338	1
Si	0.74	1.18	0.0042	1.2202	0.4611	1.0036
S	11.27	15.72	0.0896	1.1873	0.6654	1.0056
Cl	0.32	0.41	0.0026	1.1281	0.6966	1.0091
Ag	0.71	0.3	0.006	0.9398	0.8859	1.0169
Ca	0.14	0.16	0.0015	1.1579	0.8746	1.0419
Ba	67.14	21.86	0.5904	0.864	1.0177	1
Ti	4.39	4.1	0.0436	1.0623	0.9351	1
Total	100	100				

Table 2.11: EDS spot 2 analysis of elemental composition of Sikagard 62T.

Element	Wt %	At %	K-Ratio	Z	A	F
C	93.45	97.29	0.5669	1.0061	0.6029	1
O	1.37	1.07	0.002	0.9873	0.1463	1
Si	1.19	0.53	0.0104	0.9309	0.9385	1.0016
S	2.07	0.81	0.0193	0.9236	1.0072	1.0014
Cl	0.43	0.15	0.0039	0.8843	1.0083	1.0013
Ag	0.61	0.07	0.0052	0.7383	1.163	1.0008
Ca	0	0	0	0.9057	1.0254	1.0022
Ba	0.87	0.08	0.0065	0.6672	1.1182	1
Ti	0	0	0	0.8233	1.0261	1
Total	100	100				

Table 2.12: XRF analysis of elemental composition of Sikagard 62T.

Compound	Values	Unit
Al ₂ O ₃	1.15	%
SiO ₂	2.37	%
SO ₃	4.046	%
K ₂ O	0.354	%
CaO	1.04	%
TiO ₂	5.142	%
Cr ₂ O ₃	0.205	%
MnO	0.048	%
Fe ₂ O ₃	0.64	%
NiO	0.079	%
CuO	0.014	%
ZnO	0.013	%
As ₂ O ₃	0.013	%
Rb ₂ O	0.022	%
SrO	0.214	%
ZrO ₂	0.033	%
BaO	17.032	%
ThO ₂	0.127	%
U ₃ O ₈	0.025	%
Total	30.9	%
Actual Total	100.44	%

Table 2.13: C and N analysis of Sikagard 62T.

Type:	Routine
Archive:	BEAD1
Application:	BEAD1
Init Weight:	0.84g
Flux Weight:	4.5g
Final Weight:	5.34g
LOI (%):	69.54
Carbon (%):	55.71
Nitrogen (%):	1.73

2.5 Fenco S301 Ultracoat (UK)

SEM examination of Fernco S301 in Figure 2.7 shows air bubble holes. However it is apparent that the main epoxy is relatively non-porous. This is confirmed by the higher magnification (x2000) examination of the coating surface in Figure 2.8. It is also apparent from these images that the filler inclusions are very fine and are not obvious under these two images. EDS analysis (Table 2.14) suggests the fillers are Si, Ti and Ba. The quantities of the fillers are much lower in comparison to any of the Sika coating used in this study. XRF analysis in Table 2.15 confirms the presence of Si and Al. The LOI (88%) in Table 2.16 suggest the much higher proportion of epoxy in this coating in comparison to the Sika coating samples. This coating contains S (0.563% as SO₃) and N (2.69%).

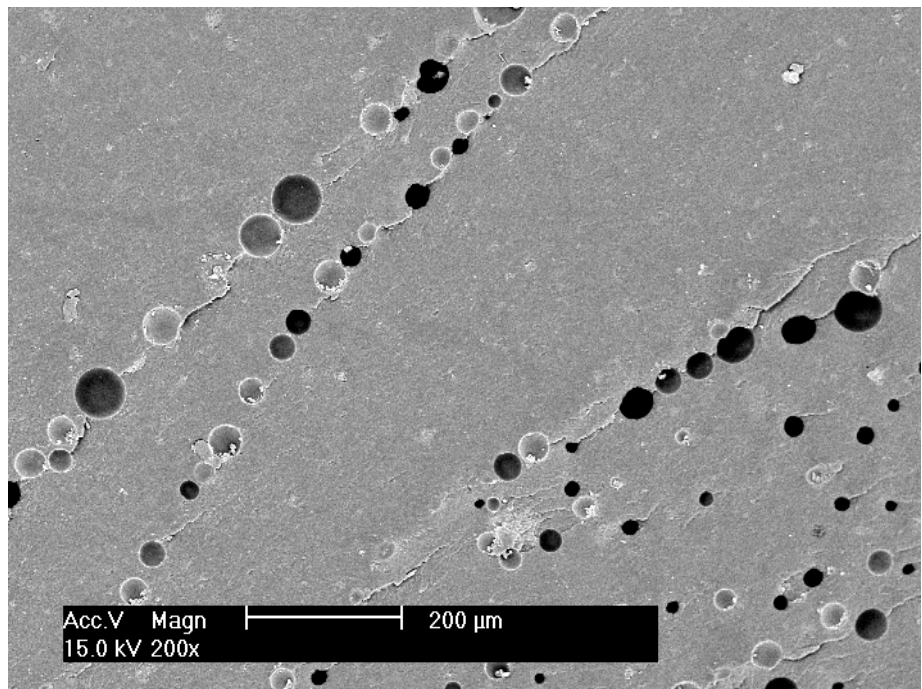


Figure 2.7: SEM image of Fernco S301 (UK).

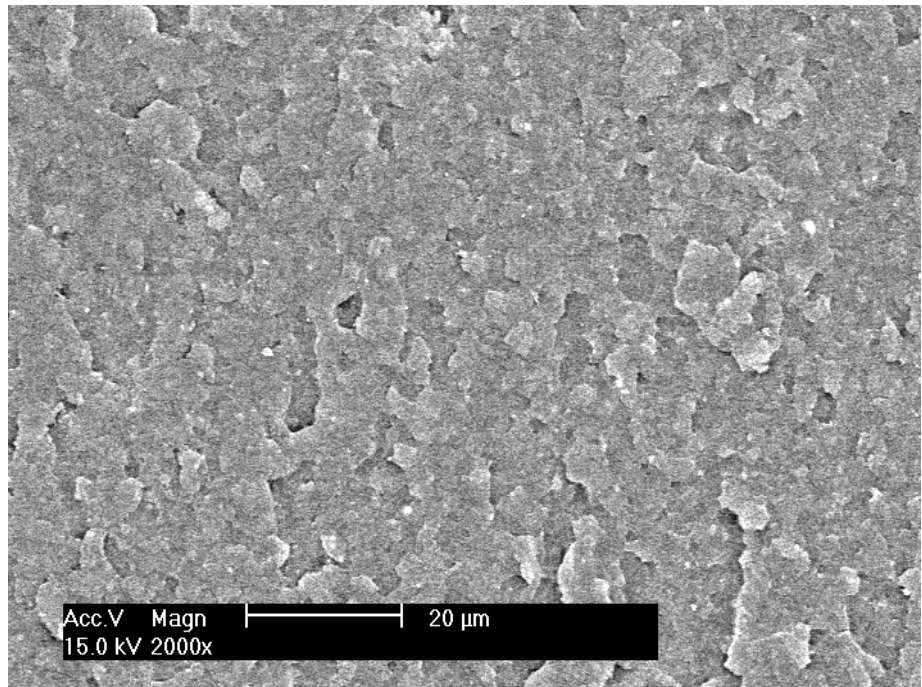


Figure 2.8: SEM image of Fernco S301 (UK).

Table 2.14: EDS average analysis of elemental composition of Fernco S301 (UK).

Element	Wt %	At %	K-Ratio	Z	A	F
C	82.13	91.66	0.3335	1.0155	0.3998	1
O	3.41	2.85	0.0051	0.9965	0.1491	1.0001
Si	7.18	3.43	0.0626	0.9409	0.9257	1.0016
S	1.29	0.54	0.0116	0.933	0.9537	1.0029
Cl	1	0.38	0.0087	0.8931	0.9751	1.0034
Ag	1.35	0.17	0.0114	0.7455	1.1274	1.0034
Ca	0.8	0.27	0.0074	0.9147	1.0063	1.0058
Ba	0.51	0.05	0.0038	0.6741	1.1004	1
Ti	2.34	0.65	0.0197	0.8318	1.0124	1
Total	100	100				

Table 2.15: XRF elemental analysis of Fernco S301 (UK).

Compound	C (%)	Unit
Al ₂ O ₃	3.08	%
SiO ₂	6.98	%
SO ₃	0.563	%
K ₂ O	0.326	%
CaO	0.79	%
TiO ₂	1.064	%
V ₂ O ₅	0.019	%
Cr ₂ O ₃	0.107	%
MnO	0.014	%
NiO	0.016	%
ZrO ₂	0.020	%
CeO ₂	0.243	%
PbO	0.017	%
ThO ₂	0.127	%
U ₃ O ₈	0.032	%
Total	13.0	%
Actual total	101.04	%

Table 2.16: C and N analysis of Fernco S301 (UK).

Type:	Routine
Archive:	BEAD1
Application:	BEAD1
Init Weight:	0.84g
Flux Weight:	4.5g
Final Weight:	5.34g
LOI (%):	88.04
Carbon (%):	79.19
Nitrogen (%):	2.69

2.6 Nitomortar ELS (Pharchem)

SEM examination of nitomortar ELS in Figure 2.9 and 2.10 shows the presence of air bubble holes and widely varying inclusions and ‘egg shaped’ inclusions that appear to contain epoxy with filler but surrounded by a shell. These are surrounded by seemingly porous substrate. The inorganic inclusions appear to consist of both spherical and dense rectangular shaped (100x50µm) shaped edge solids. EDS analysis in Table 2.16 suggests the main filler is Si; confirmed by the XRF analysis in Table 2.17. The LOI (59%, Table 2.18) suggests the proportion of epoxy in this coating is between the Sikagard 62T and Sikadur 41. The coating contains S (0.526% as SO₃) and N (1.5%) (Tables 2.17 and 2.18).

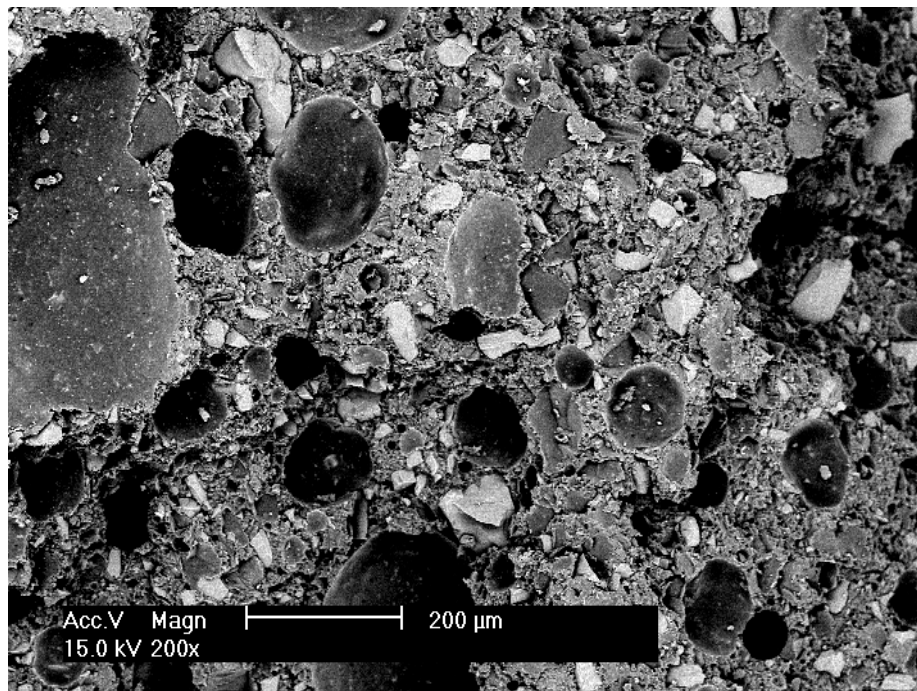


Figure 2.9: SEM image of Nitomortar ELS(Pharchem).

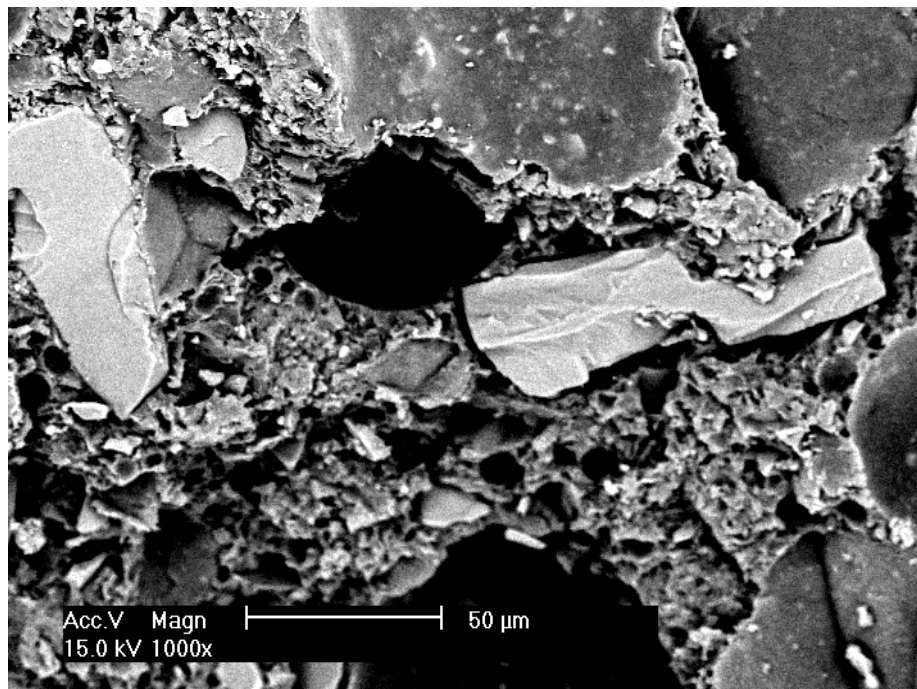


Figure 2.10: SEM image of Nitomortar ELS(Pharchem).

Table 2.17: EDS average analysis of elemental composition of Nitomortar ELS(Pharchem).

Element	Wt %	At %	K-Ratio	Z	A	F
C	6.05	12.71	0.0054	1.0706	0.0841	1.0001
O	10.02	15.8	0.0219	1.0501	0.2082	1.0006
Si	75.29	67.62	0.6961	1.0004	0.9233	1.001
S	1.85	1.45	0.0107	0.9882	0.5865	1.0013
Cl	1.26	0.89	0.008	0.9445	0.676	1.0015
Ag	3.48	0.81	0.0237	0.7881	0.8648	1.0005
Ba	1.1	0.2	0.0079	0.7144	1.0062	1
Ti	0.97	0.51	0.0079	0.8811	0.9253	1
Total	100	100				

Table 2.18: XRF elemental analysis of Nitomortar ELS(Pharchem).

Compound	D (%)	Unit
MgO	1.61	%
Al ₂ O ₃	0.31	%
SiO ₂	36.56	%
SO ₃	0.526	%
K ₂ O	0.262	%
CaO	0.68	%
TiO ₂	0.502	%
V ₂ O ₅	0.013	%
Cr ₂ O ₃	0.109	%
MnO	0.015	%
Fe ₂ O ₃	0.22	%
NiO	0.131	%
CeO ₂	0.159	%
PbO	0.011	%
ThO ₂	0.085	%
U ₃ O ₈	0.024	%
Total	41.3	%
Actual total	100.56	%

Table 2.19: C and N analysis of Nitomortar ELS(Pharchem).

Type:	Routine
Archive:	BEAD1
Application:	BEAD1
Init Weight:	0.84g
Flux Weight:	4.5g
Final Weight:	5.34g
LOI (%):	59.24
Carbon (%):	44.27
Nitrogen (%):	1.51

Appendix 3 Fourier Transform Infrared Spectroscopy (FTIR)

3.0 Fourier Transform Infrared Spectroscopy (FTIR)

3.1 Summary of Results

FTIR provides surface functional group analysis. Surface functional groups reflect the surface chemistry of the epoxy. For example hydroxyl group ($-OH$), carboxyl group ($C=O$), sulphate and sulfonate groups ($S=O$) and amino group ($N-H$) that have unpaired electron, epoxy has exhibited the hydrophilic properties by attracting water from the environment to which it is exposed. The higher uptake of moisture will reduce the effectiveness of the coating in acting a barrier to corrosive environments.

A summary of the FTIR analysis of the coatings is shown in the Table 3.1. As shown, the main filler in Sikadur 41, Sikagard 63N , Fernco S301 and Nitomortar ELS are silica based most likely SiO_2 . FTIR revealed that silica is present both as an oxide $Si-O-Si$ and $Si-C$ reflecting the interaction of the silica filler with the epoxy. This interaction has been suggested to provide the coating with better resistance to acid and water transport. Apart from providing tortuous pathway, the link may further reduce the permeation of acid through the coating. This will be assessed in the acid permeation tests. Comparison of the ratio of $Si-C$ to the $Si-O-Si$ is shown at the bottom of the Table Band the ranking of terms of this ratio is : Fernco S301>Sikadur 41 and Sikadur 63N>Nitomortar. FTIR analysis of Sikagard 62 T revealed also the presence of $BaTiO_3$ and $C-O-Ba$ groups, reflecting also the interaction of this filler with the epoxy. The ratio of the $C-O-Ba$ to $BaTiO_3$ is shown to be 0.922 and it is apparent that the minor Ti and Si present in this coating have also form $Ti-C$ and $Si-C$ groups. Thus the overall ranking in terms of the metal-C group to filler oxides is: Fernco S301 > Sikagard 62T> Sikadur 41 and Sikadur 63N>Nitomortar.

Table 3.1: Summary of FTIR Analysis of Epoxy Coatings

Wavenumber (cm ⁻¹)	Vibrations	Sikadur 41	Sikagard 63N +Sikadur 41	Sikagard 62T	Fernco S301	Nitomortar ELS
% Normalised Relative Heights						
3390	O-H stretch			11.5	9.6	9.6
2956	Asymmetric stretching CH ₃ groups in – Si(CH ₃) ₂ –				17	
2919-2887	C-H stretch methylene			54.3	18.4	19.8
2364 - 2353	S-H stretching	4.5	18.4	6	14.2	7.9
2019	Si-H stretch	3.5	1.6			
1608 -1508	C=O-O carboxylate ion, aromatic band stretching	0.7	0.2	72.6	26	11.6
1570	Ba-C			8.5		
1246 and 1463	CH ₃ symmetric deformation of Si-CH ₃	17.3	15	36.6	75.7	56.8
1188	stretching of SO ₂	54.6		85.2		
1091	C-O-Ba			92.2		
1168, 1089	C=S and C=O	99	54.4			
1060-1039	Si-O-Si stretching vibration	100	100	88.2	76.8	100
980	Ti-C			44.8		
950	Al-O				34.2	
875	Si-OH	37.6	33.3			
830 and 657	TiO ₂			83.8		
827	Si-C stretching and rocking	86	78.9	41.7	100	62.1
732 and 636	C-H out of plane bending for aromatics	56	85.7	66.3	45.6	68
615	BaTiO ₃ (Yan, Liao et al. 2008)			100		
Ratio of Metal-C/Metal Oxide (main filler)		0.86	0.789	0.922	1.30	0.621

3.2 Sikadur 41

FTIR analysis in Figure 3.1 of Sikadur 41 and the corresponding band assignments in Table 3.1, show strong Si-O-Si (1080 cm^{-1}) band and Si-C (798 cm^{-1}). This suggests the main SiO_2 filler is present both as un-reacted oxides and reactive components of the epoxy. Weak peaks at 2368 cm^{-1} and 1188 cm^{-1} reflects S based functional groups. Although nitrogen was detected by C-N analysis, no nitrogen groups were observed in this FTIR. The normalised peak heights, which is the ratio of the assigned peak height to the maximum height in the spectra is shown in Table 3.1. The relative normalised height of the reacted Si-C is 86% of the Si-O-Si showing modest amount to interaction between the filler and epoxy.

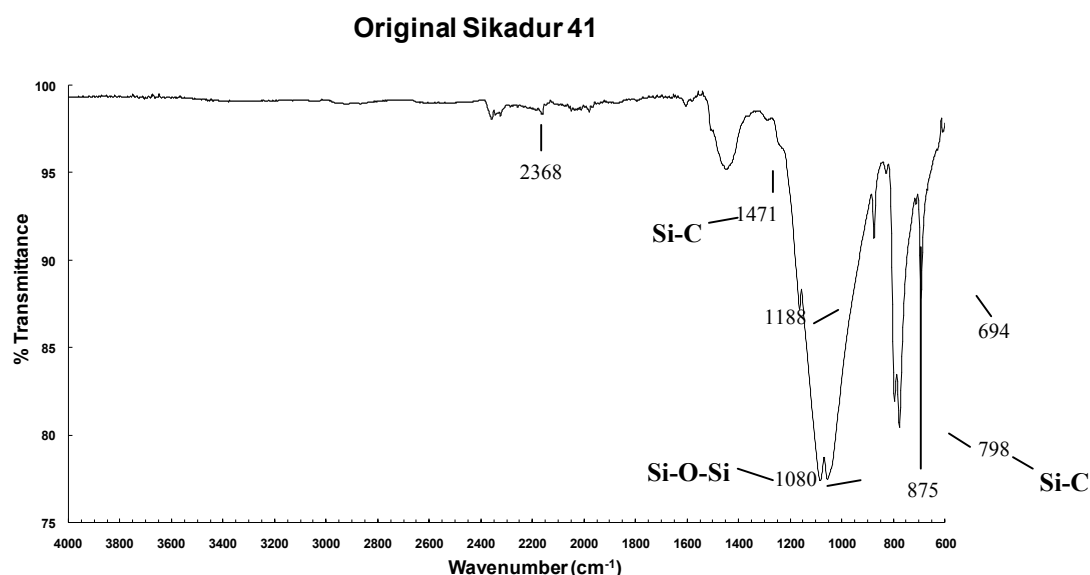


Figure 3.1: FTIR spectrum of the raw Sikadur – 41 coating

Inorganic components: SiO_2 (83%), CaO (2.9%), SO_3 (0.11%) and N (0.37%).

Table 3.2: Absorption band analysis in the IR analysis of Sikadur 41

Wavenumber (cm^{-1})	Assignments	Normalised %Height
2368 and 2189	S-H stretching	4.5
2019	Si-H stretch	3.5
1600	aromatic band stretching C-C	0.7
1251 and 1471	CH_3 symmetric deformation of Si-CH₃	17.3
1188	stretching of SO ₂	54.6
1168, 1089	C=S and C=O	99.0
1080	Si-O-Si stretching vibration	100.0
875	Si-OH	37.6
798	Si-C stretching and rocking	86.0
779 and 694	C-H out of plane bending for aromatics	56.0

3.3 Sikagard 63N and Sikadur 41

The FTIR analysis of Sikagard 63N and Sikadur 41 in Figure 3.2 and its corresponding band assignment in Table 3.3 show similar features to Sikadur 41 alone (Figure 3.1). The relative height of Si-C to Si-O-Si (78%) is comparable to Sikadur 41 alone.

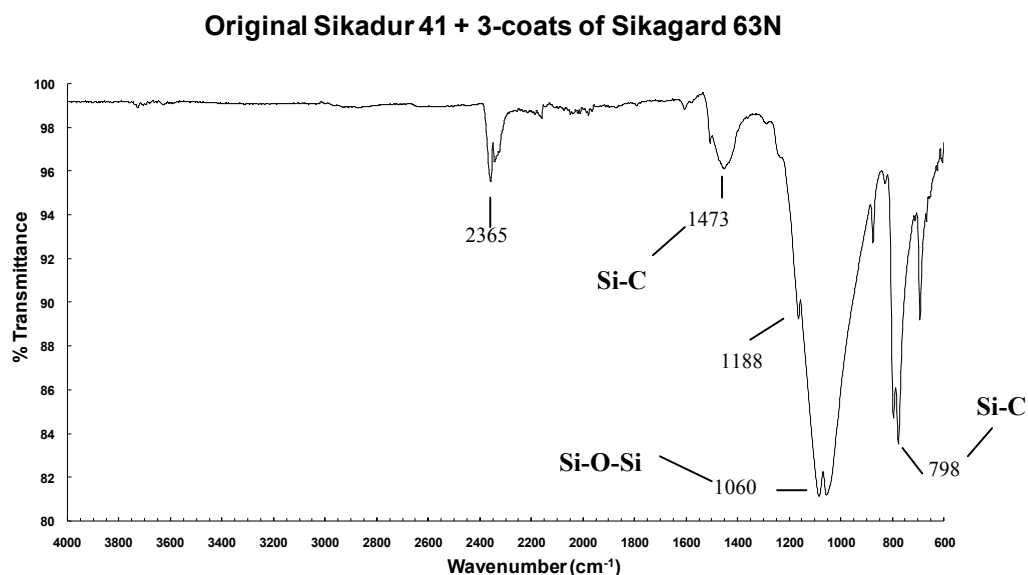


Figure 3.2: FTIR spectrum of the raw Sikadur – 41 with 3 coats of 63N coating

Inorganic components: SiO₂ (41.6%), TiO₂ (2.9%), CaO (1%), SO₃ (0.409%) and N (1.55%).

Table 3.3: Absorption band analysis in the IR analysis of Sikagard 63N + Sikadur 41

Wavenumber (cm ⁻¹)	Assignments	Normalised %Height
2365 and 2345	S-H stretching	18.4
2019	Si-H stretch	1.6
1615	aromatic band stretching C-C	0.2
1249 and 1473	CH ₃ symmetric deformation of Si-CH ₃	15.0
1166, 1091	C=S and C=O	54.4
1080	Si-O-Si stretching vibration	100.0
877, 830	Si-OH, TiO ₂	33.3
798	Si-C stretching and rocking	78.9
779, 694	C-H out of plane bending for aromatics	85.7

3.4 Sikagard 62T

The Sikagard 62T (Figure 3.3) and the corresponding band assignment in Table 3.3 shows this coating has a complex mixture of functional and metal-organic groups. The FTIR bands suggests free BaTiO₃ (barium titanate) and TiO₂ fillers. It is also apparent that the Ba and Ti metals have also interacted with the epoxy group. The direct interaction of the metals with the epoxy as Ba-C (1570 cm⁻¹) and Ti-C (980 cm⁻¹) groups are represented by weak bands. The interaction of Ba-O-C (1090 cm⁻¹) is stronger suggesting the metals may be reacting directly with the oxide functional groups on the epoxy surface. Sikagard 62T is also shown to have O-H groups (3371 cm⁻¹) which would make this surface hydrophilic and epoxy coating also contains strong C=C groups (2918-2850 cm⁻¹) and Si-O-Si (1030 cm⁻¹). The normalised % height for the various bands in Sikadur 62T is reported in Table 3.2. As shown the relative ratio of Ba-O-C to BaTiO₃ is the high is 92.2% again demonstrating modest reaction of the filler and epoxy. The Ti-C and Si-C ratios to their oxides are about 50%. Overall there are greater interactions between the filler and epoxy in Sikadur 62T than in Sikadur 41 and Sikagard 63N.

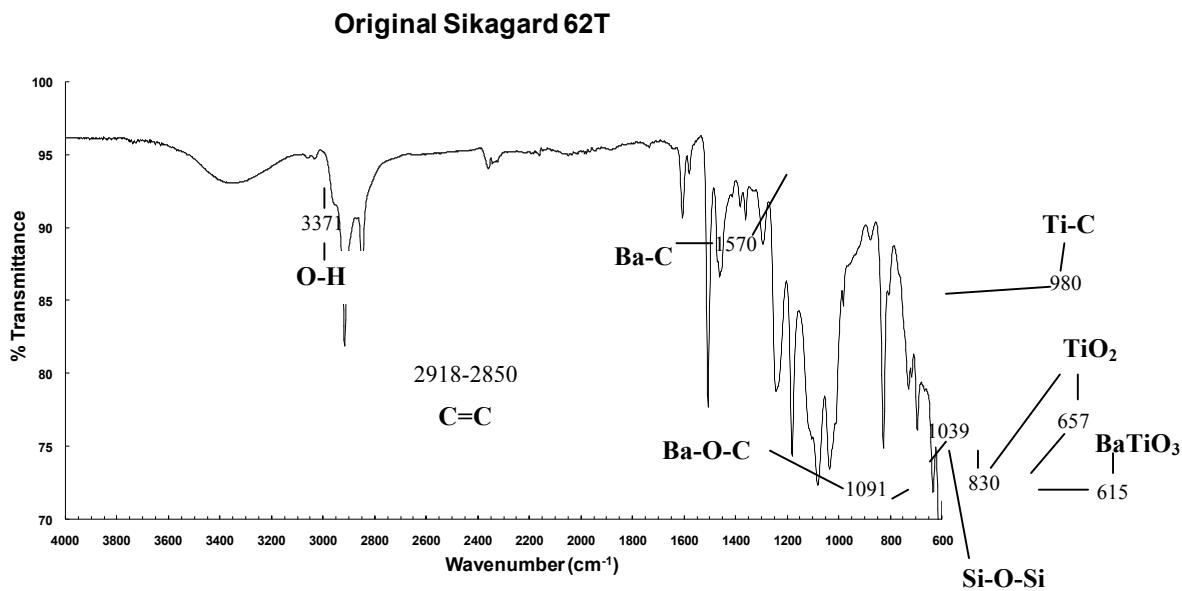


Figure 3.3: FTIR spectrum of the raw Sikagard 62T coating.

Inorganic components: BaO (17%), TiO₂ (5.1%), SiO₂ (2.37%), Al₂O₃ (1%), CaO (1%), SO₃ (4.05%) and N (1.73%).

Table 3.4: Absorption band analysis in the IR analysis of Sikagard 62T.

Wavenumber (cm ⁻¹)	Assignments	Normalised %Height
3371	O-H stretch	11.5
2918-2850	C-H stretch methylene	54.3
2370 and 2353	S-H stretching	6.0
1608 -1510	C=O-O carboxylate ion	72.6
1570	Ba-C	8.5
1247 and 1463	CH ₃ symmetric deformation of Si-CH ₃	36.6
1182	stretching of the SO ₂	85.2
1091	C-O-Ba	92.2
1039	Si-O-Si stretching vibration	88.2
980	Ti-C	44.8
830 and 657	TiO ₂	83.8
813	Si-C stretching and rocking	41.7
732, 694	C-H out of plane bending for aromatics	66.3
615	BaTiO ₃ (Yan et al. 2008)	100.0

3.5 Fernco S301

The FTIR spectra of Fernco S301 (Figure 3.4) and the corresponding assignments in Table 3.5 shows two distinct features- the relatively higher Si-C peak (827cm^{-1}) in comparison to the Si-O-Si peak (1039 cm^{-1}) and the Si-C peak in 2956 cm^{-1} assigned to the interaction of Si-CH₃. Both these features suggest a stronger interaction between the SiO₂ filler and the epoxy. There is also Al-O group (950 cm^{-1}) but it is present as a very weak peak and O-H at 3390 cm^{-1} . As shown in Table 3.5, the relative ratio of the Si-C band to Si-O-Si is 130% which is higher than all the coating used in this study.

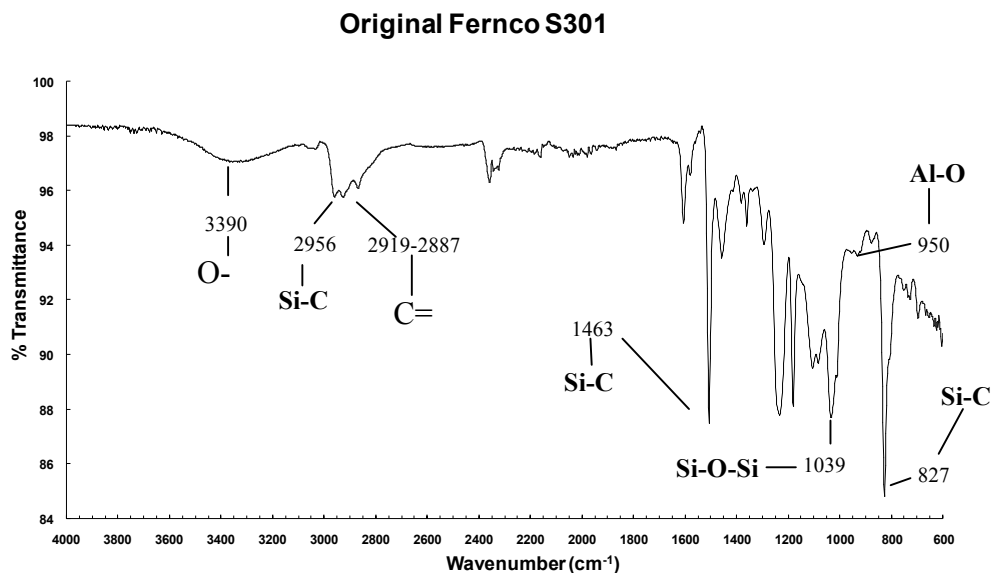


Figure 3.4: FTIR spectrum of the raw Fernco S301 coating.

Inorganic components: SiO₂ (7%), Al₂O₃ (3%), TiO₂ (1%), SO₃ (0.56%) and N (2.69%).

Table 3.5: Absorption band analysis in the IR analysis of Fernco S301.

Wavenumber (cm ⁻¹)	Assignments	Normalised %Height
3390	O-H stretch	9.6
2956	Asymmetric stretching CH ₃ groups in –Si(CH ₃) ₂ – (Simor et al. 2007)	17.0
2919-2887	C-H stretch methylene	18.4
2364 - 2353	S-H stretching	14.2
1608 -1508	C=O-O carboxylate ion	26.0
1246 and 1463	CH ₃ symmetric deformation of Si-CH ₃	75.7
1060-1039	Si-O-Si stretching vibration	76.8
950	Al-O	34.2
827	Si-C stretching and rocking	100.0
732 and 636	C-H out of plane bending for aromatics	45.6

3.6 Nitomortar ELS

A distinct feature of the Nitomortar spectra in Figure 3.5 and its corresponding assignment of bonds is the relatively lower ratio of Si-C (800 cm⁻¹) to Si-O-So (1082-1012 cm⁻¹). This suggests the filler in this epoxy material are present primarily as free fillers and only a relatively lower proportion of the filler has reacted with the epoxy. MgO bands are reflected at 1612 cm⁻¹ but no interaction with the epoxy was evident. This coating also contains O-H at 3390 cm⁻¹. The relative % heights reported in Table 3.6 shows the ratio of Si-C to Si-O-Si is 62.1% which is perhaps the lowest among the coatings used in this study.

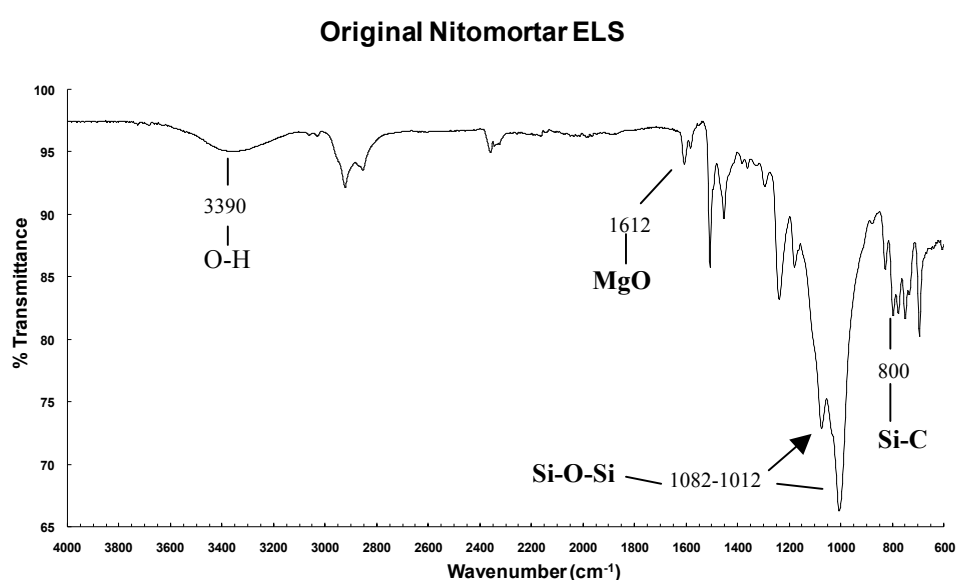


Figure 3.5: FTIR spectrum of the raw Nitomortar ELA coating

Inorganic components: SiO₂ (36%), MgO (1.6%), SO₃ (0.53%) and N (1.5%).

Table 3.6: Absorption band analysis in the IR analysis of Nitomortar ELS.

Wavenumber (cm ⁻¹)	Assignments	Normalised %Height
3390	O-H stretch	9.6
2929-2887	C-H stretch methylene	19.8
2368-2351	S-H stretching	7.9
1612 -1510	C=O-O carboxylate ion, MgO (Borchert et al. 2007)	11.6
1244 and 1456	CH ₃ symmetric deformation of Si-CH ₃	56.8
1082-1012	Si-O-Si stretching vibration	100.0
800	Si-C stretching and rocking	62.1
700	C-H out of plane bending for aromatics	68.0

3.7 Polibrid 705E

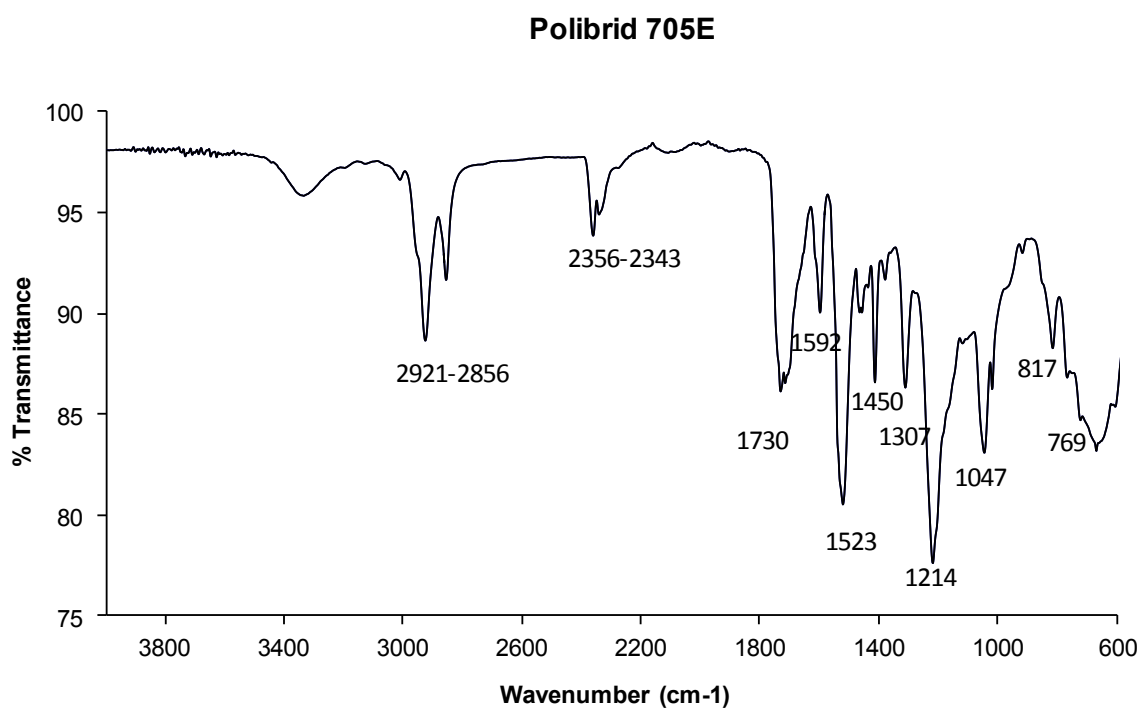


Figure3.6 FTIR spectrum of the raw Polibrid 705E coating.

Table 3.7. Absorption band analysis in the IR analysis of Polibrid 705E.

Wavenumber (cm ⁻¹)	Assignments	Normalised %Height
3328	N-H stretching	18.7
2921-2856	Asymmetric stretching CH ₃ groups in -Si(CH ₃) ₂	50.8
2356 - 2343	CH ₂ and CH ₃ stretch methylene	26.9
1730	C=O, amine stretching , non-bonded urethane stretching	62.7
1523	NH, amide deformation	86.2
1450	CH ₂ , scissor	41.5
1307	OCOCH, wagging	61
1214		100
1047	OCONH, in plane vibrations	75.5
817	CH ₂ pendulum swing	51.9

3.8 Hychem TL5

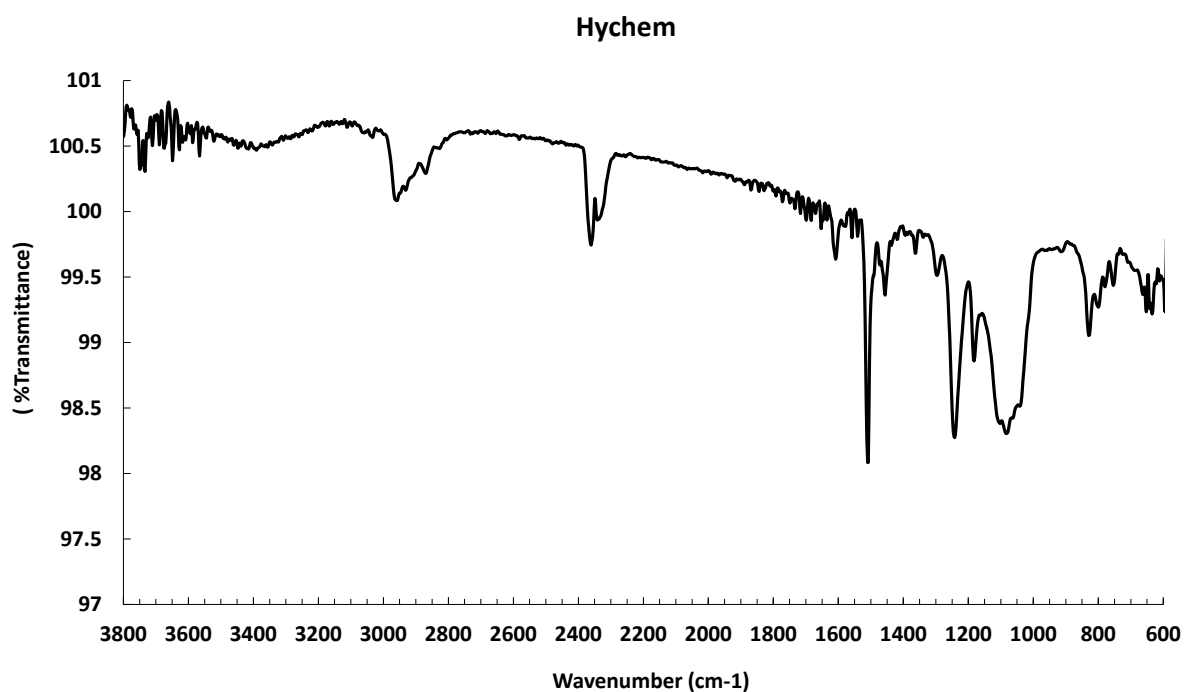


Figure 3.7 FTIR spectrum of the raw Hychem TL5 coating.

Table 3.8. Absorption band analysis in the IR analysis of Hychem TL5.

Wavenumber (cm ⁻¹)	Vibrations	Hychem LT5
3390	O-H stretch	18.36
2956	Asymmetric stretching CH ₃ groups in Si(CH ₃) ₂ –	27
2919-2887	C-H stretch methylene	
2364 - 2353	S-H stretching	28.2
2019	Si-H stretch	
1608 -1508	C=O-O carboxylate ion, aromatic band stretching	30.2, 66.1
1570	Ba-C	
1246 and 1463	CH ₃ symmetric deformation of Si-CH ₃	81.3
1188	stretching of SO ₂	
1091	C-O-Ba	
1168, 1089	C=S and C=O	
1060-1039	Si-O-Si stretching vibration	100
980	Ti-C	
950	Al-O	
875	Si-OH	
830 and 657	TiO ₂	
827	Si-C stretching and rocking	81.7
732 and 636	C-H out of plane bending for aromatics	70.7
Ratio of Metal-C/Metal Oxide (main filler)	SiC/Si-O-Si	0.817

Appendix 4 Thermogravimetric analysis of coatings

4.0 Thermogravimetric analysis of coatings

Thermal gravimetric analysis measures the weight loss of a sample as it is heated at a certain temperature ramp rate. Differential plot of the weight loss curve will show the weight lost areas as peaks. Any loss of weight is associated with chemical reactions or structural damage of the sample. If there is some structural degradation, the bonding strength of the material will be reduced. As such the thermal degradation temperature of the epoxy will also be reduced. Often if new components results from the degradation new weight loss areas (or DTA peaks) will be observed. With post-polymeriation there will be higher degradation temperature.

4.1 Summary of Results

Thermogravimetric profiles of epoxy based coatings reflects the molecular weight of the resin components and the also the extent of crosslinking and interaction between inorganic fillers with epoxy.

Future testing of the coating will be used to examine the effect of moisture uptake and acid uptake on the epoxy. The modification in thermal decomposition temperature T_d , define here as the temperature of optimum weight loss of the epoxy as a result of temperature treatment. T_d is most likely to also relate to the glass transition temperature of the epoxy. During immersion the reduction in T_d reflects the degree of polymer matrix plasticization and water/resin interactions. T_d value of organic coating was usually found to decrease after immersion because the absorbed water molecules may disrupt the inter-chain hydrogen bonds. Such effects are likely to be enhanced in epoxy exposed to acidic environments.

A summary of the thermogravimetric results are given in Table 4.1 below.

Table 4.1: Thermal decomposition temperatures of coatings

		Thermal degradation temperature (°C)					
Attributed weight loss (%)	Pure Epoxy	Coatings with Inorganic Fillers					
		Sikadur 41	Sikagard 63 + Sikadur 41	Sikagard 62T	Fernco S301	Nitomortar ELS	
Moisture + uncured resin		105	105	148	165	138	
Filler-Epoxy	350	360	360	370	377	370	
Dehydroxylation of Filler		715	675,715	478			
		Weight Loss (wt%)					
Filler-Epoxy		7.5	12.12	50.05	73.28	50	

It has been shown that the filler can affect the the Td of the epoxy. The grafting of the filler with the resin will restrict the movement of polymer and the degradation of the polymers at high temperatures resulting in higher Td values(Borchert, Jurgens et al. 2007; Hong, Fu et al. 2007; Ohman and Persson 2007; Chandradass and Bae 2008; Gisdavic-Nikolaidis, Edmonds et al. 2008; Tsai, Lu et al. 2008; Yan, Liao et al. 2008). The typical degradation of epoxy is around 350 °C and as shown in Table 4.1, the degradation temperature of the epoxy with filler is increased. The higher temperature of degradation around this temperature is indicative of the extent of crosslinking between the filler and epoxy. Based on the result shown in the summary Fernco S301 provides both the highest temperature of degradation and the highest quantity of crosslinked epoxy-filler followed by both Sikagard 62T and Nitomortar ELS. The Sikadur 41 and Sikagard 63 providing also some crosslinking with the filler but at the lower temperatures and lower concentration of filler-epoxy groups. The difference in filler-epoxy group attributed to Sikagard 63N is about 60% of that in Sikadur 41 alone. Since in the composite coating Sikagard is only present as 3 coatings being equivalent to 150 µm. This suggest the presence of the filler-epoxy group in Sikagard 63N is also very high. The result for Nitomortar is surprising because its FTIR suggested a relatively higher Si-O-Si group than Si-C band. These results seem to suggest that the smaller Si-C interaction in this coating is sufficient to adjust its degradation temperature to 370°C making it a favourable coating.

4.2 Sikadur 41

The TGA analysis (weight loss vs temperature) of Sikadur 41 is shown in Figure 4.1. Superimposed on this graph is the derivative of the thermogram showing three distinct weight loss at 105, 360 and 715 °C (Table 4.1). The temperatures are located at the derivative peaks. The low temperature endothermic peak is most likely to be associated with loss of water and any solvent residue. The T_d at 360°C is attributed to the decomposition of silicate-epoxy polymer and the higher T_d (715°C) to the dehydrolylation of the filler. Gizdavic-Nikolaidis et al (Gizdavic-Nikolaidis, Edmonds et al. 2008) has shown the decomposition to SiO_2 occurs at about 700°C, which is consistent with our observation in Figure 4.1.

The relative weight of the water and epoxy that would evolve with thermal degradation was estimated as follow assuming the T_d 715°C is associated with decomposition of $\text{SiO}_2\cdot\text{H}_2\text{O}$:

Based on 100 gram of epoxy

Mass of epoxy based on LOI = 18 grams

Mass of filler: 82 grams

Molecular weight of SiO_2 = 60 g/mole

Molecular weight of H_2O = 18 g/mole

$$\text{Weight of water removed at } 715 \text{ } ^\circ\text{C} = 18/(18+60)*82 = 18 \text{ grams}$$

The relative weight loss between the epoxy and from $\text{SiO}_2\cdot\text{H}_2\text{O}$ expected to be 1.0:1.0, which is consistent with the weight loss observed between 360 and 715°C of 1.1:1.0. This adds further support of the decomposition at 715°C is associated with $\text{SiO}_2\cdot\text{H}_2\text{O}$.

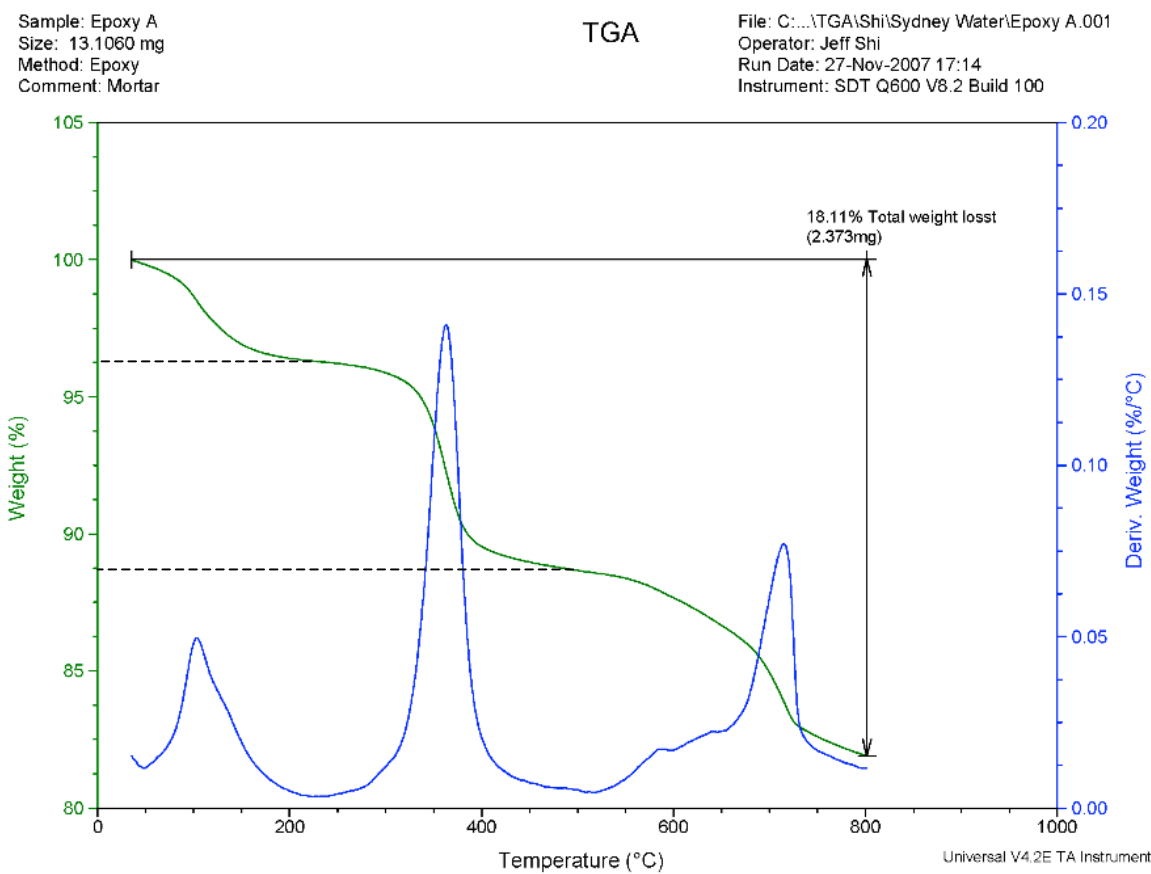


Figure 4.1: TGA thermogram of Sikadur 41.

Table 4.2: Thermal decomposition regions in Sikadur 41.

Optimum Degradation Temperature (°C)	Weight Loss (wt%)	Attributed Weight Loss
105	3.75	Moisture
360	7.5	Epoxy-Silicate
715	6.86	Dehydroxylation of the SiO ₂ H ₂ O

4.3 Sikadur 63N and Sikadur 41

The TGA thermogram of a composite of Sikagard 63N and Sikadur 41 is shown in Figure 4.2. The temperature of decomposition at 105, 360, 675 and 715 °C are reported in Table 4.2. These degradation temperatures are similar to that shown in Figure 4.1 as would be expected because of the Sikadur content of this coating. The low temperature degradation at 105°C is attributed to moisture loss. The additional degradation temperature at 675°C is attributed to Sikagard 63N. The main difference in Sikadur 41 and Sikagard 63N is the presence of TiO₂ in Sikagard 63N. It is likely the 675°C endotherm is associated with the TiO₂ dehydroxylation. The relatively higher T_d observed here at 365 °C could be associated with the additional grafting of the TiO₂ filler with the epoxy.

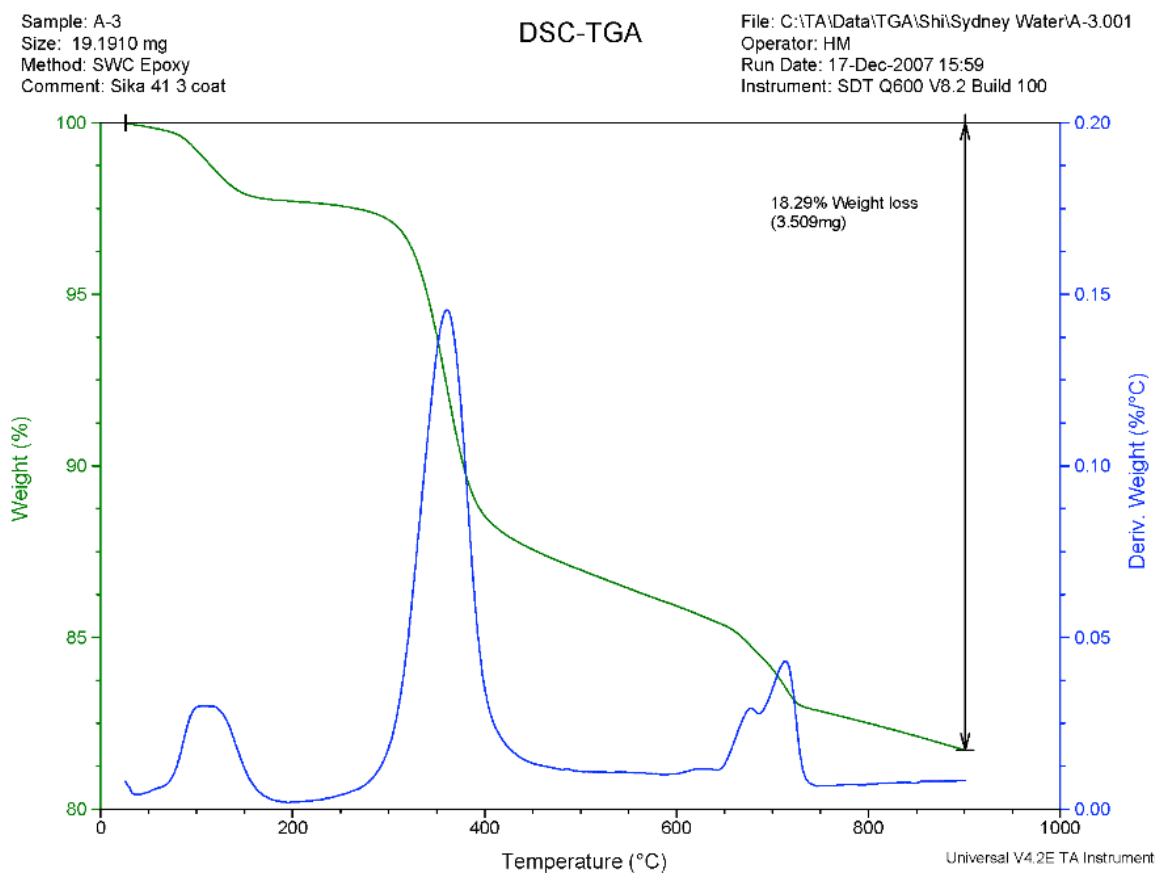


Figure 4.2: TGA thermogram of Sikagard 63N and Sikadur 41.

Table 4.3: Thermal decomposition regions in Sikadur 41.

Optimum Degradation Temperature (°C)	Weight Loss (wt%)	Attributed Weight Loss
105	2.25	Moisture
360	12.12	Epoxy-Silicate
675	1.25	Dehydroxylation of TiO ₂ .H ₂ O
715	2.665	Dehydroxylation of the SiO ₂ H ₂ O

4.4 Sikagard 62T

The TGA thermogram of Sikagard 62T is shown in Figure 4.3. The degradation temperatures and the corresponding weight loss are summarised in Table 4.4. As show degradation occurred at three distinct temperatures at 148, 370, 478 °C. The peak at 148 °C appear to consist of two peaks that have merged. The lower of these peak is attributed to moisture loss and higher to un-cured epoxy or residual epoxy component. The peak 370°C is attributed to the decomposition of the epoxy-BaTiO₃. The typically degradation of epoxy is around 350 °C and addition of barium titanate can increase the temperature of degradation by 10°C Chandradass and Bae (Chandradass and Bae 2008) has suggested pure cured epoxy degrades at 350 °C and grafting 5% BaTiO₃ increased this temperature of degradation by 9°C. XRF analysis of this coating contains 17% BaTiO₃ and the partial grafting of this filler have resulted in the higher observed degradation temperature in this coating of 370°C. Chandradass and Bae (2008) has also observed a second thermal degradation at 546°C in epoxy containing BaTiO₃. This temperature was found to increase with BaTiO₃ suggesting this is partially an interaction of the epoxy and the filler. In this coating, however this was only observed at 478 °C.

Sample: SWC Epoxy Sample B
Size: 16.4900 mg
Method: SWC Epoxy

TGA

File: C:\TGA\Shi\Sydney Water\Epoxy B.001
Operator: J Shi
Run Date: 10-Dec-2007 16:49
Instrument: SDT Q600 V8.2 Build 100

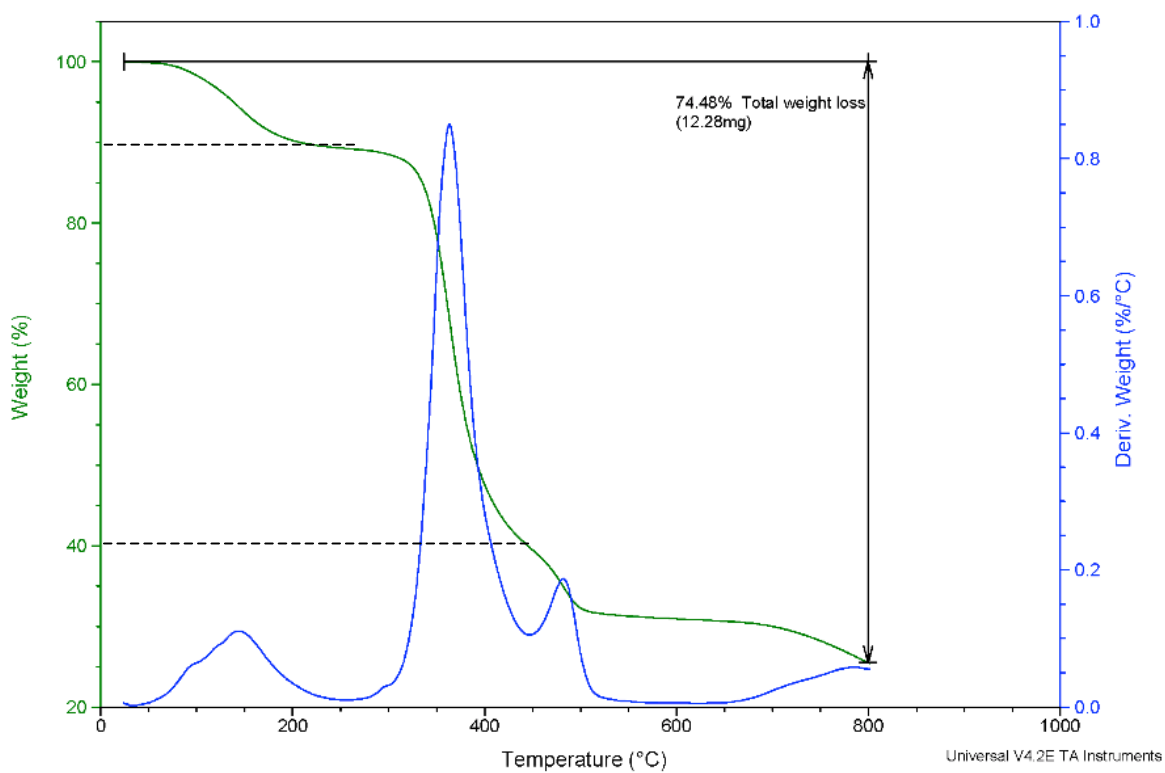


Figure 4.3: TGA thermogram of Sikagard 62T.

Table 4.4: Thermal decomposition regions in Sikagard 62T.

Optimum Degradation Temperature (°C)	Weight Loss (wt%)	Attributed Weight Loss
148	10	Moisture and uncured epoxy
370	50.05	Epoxy-Barium Titanate
478	14.43	Epoxy-Barium Titanate

4.5 Fernco S301

The TG thermogram of Fernco S301 is shown in Figure 4.4. The correponding thermal decomposition temperatures and weight losses are reported in Table 4.5. These occurred at 165 and 377 °C. The low exothermic peak at Td of 165 °C is attributed to uncured epoxy and 377°C to the grafting of SiO₂ with the epoxy. This is relatively higher in comparison the the Sika samples suggesting the higher crosslinking of the filler with the epoxy. This is confirmed by the FTIR analysis which suggested a greater interaction between the filler and epoxy. The lack of other peaks at the higher temperature suggest most of the filler are cross linked with the epoxy. The lack of thermal decomposition at higher temperature suggests the Si filler is not hydrated or do not have molecularly bound water.

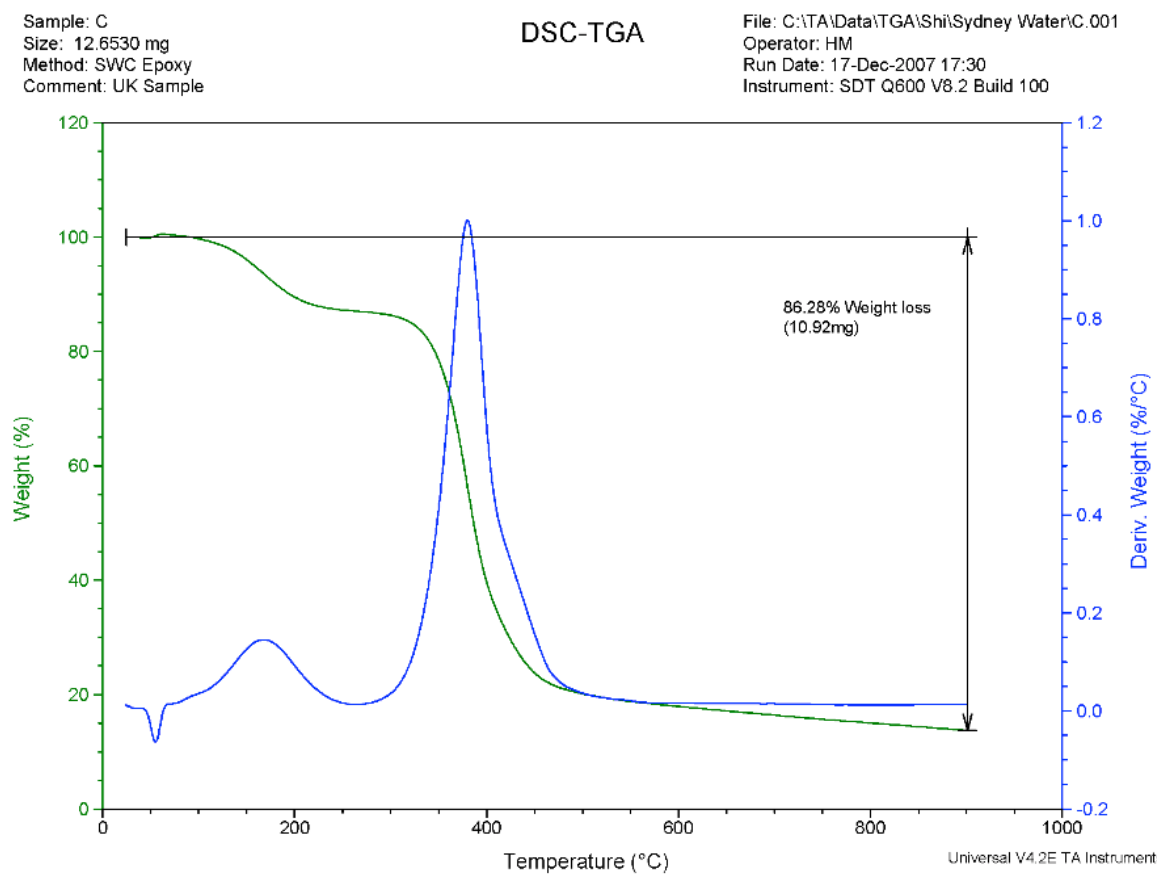


Figure 4.4: TGA thermogram of Fernco S301.

Table 4.5: Thermal decomposition regions in Fernco S301.

Optimum Degradation Temperature (°C)	Weight Loss (wt%)	Attributed Weight Loss
165	13	uncured epoxy
377	73.28	Epoxy-SiO ₂

4.6 Nitomortar ELS

The TG thermogram of Nitomortar ELS is shown in Figure 4.5. The correponding thermal decomposition temperatures and weight losses are reported in Table 4.6. These occurred at 138 and 370 °C. The low temperature degradation at 138°C is attributed to moisture loss and un-cured epoxy. The higher temperature of degradation at 370 °C, is attribued to high crosslinking of SiO₂ with the epoxy. This is somewhat surprising because FTIR analysis suggested this coating showed weak Si-C group. The lack of thermal decomposition at higher temperature suggests the Si filler is not hydrated or do not have molecularly bound water.

Sample: SWC Epoxy Sample D
Size: 15.0420 mg
Method: SWC Epoxy

TGA

File: C:\TGA\Shi\Sydney Water\Epoxy D.001
Operator: J Shi
Run Date: 10-Dec-2007 18:02
Instrument: SDT Q600 V8.2 Build 100

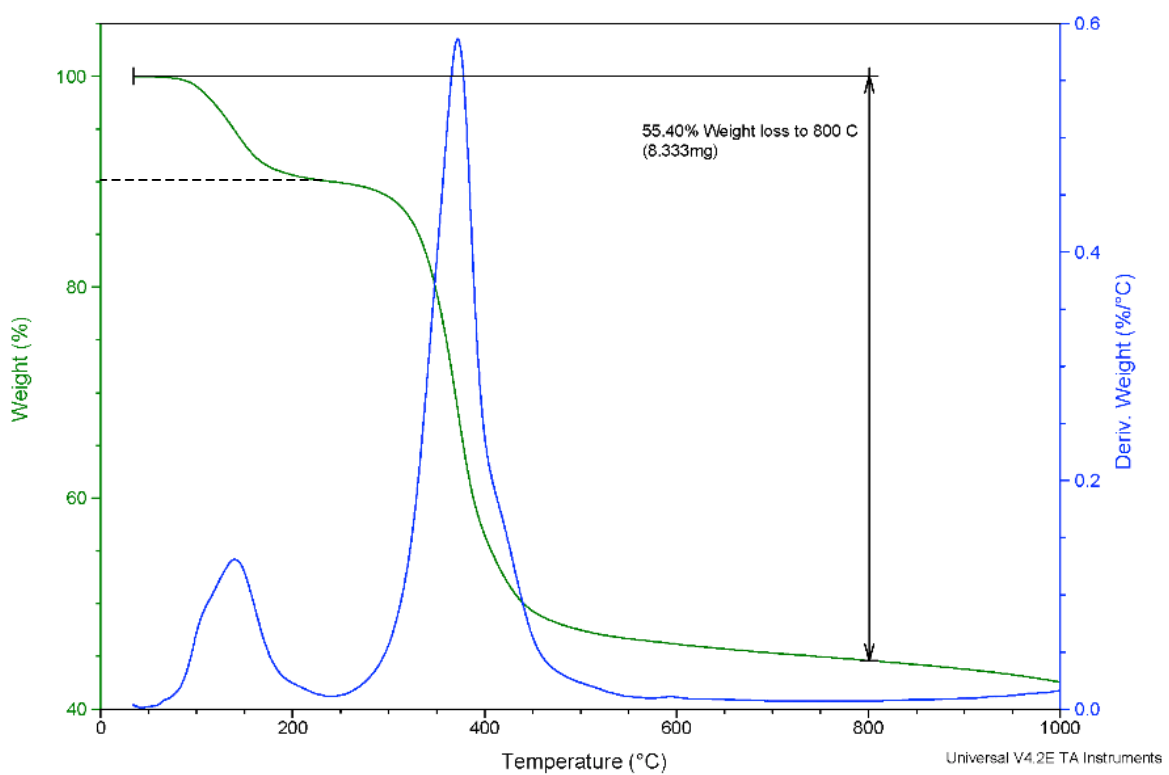


Figure 4.5: TGA thermogram of Nitomortar ELS.

Table 4.6: Thermal decomposition regions in Nitomortar ELS.

Optimum Degradation Temperature (°C)	Weight Loss (wt%)	Attributed Weight Loss
138	10	Moisture and uncured epoxy
370	50	Epoxy-SiO ₂

4.7 Hychem TL5

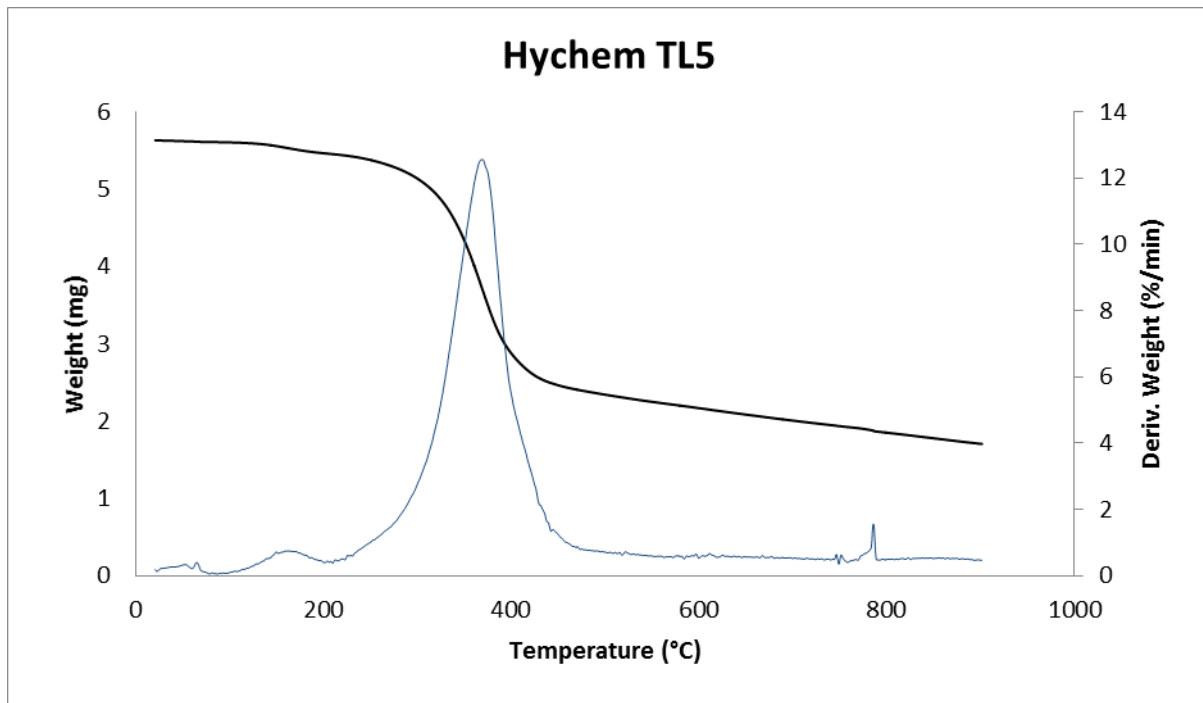


Figure 4.6: TGA thermogram of Hychem TL5

Table 4.7: Thermal decomposition regions in Hychem TL5

Optimum Degradation Temperature (°C)	Weight Loss (wt%)	Attributed Weight Loss
165	2.66	Uncured epoxy
369.2	55.5	Epoxy-SiO ₂

5.0 Differential Scanning Calorimetry (DSC)

5.1 Fernco S301

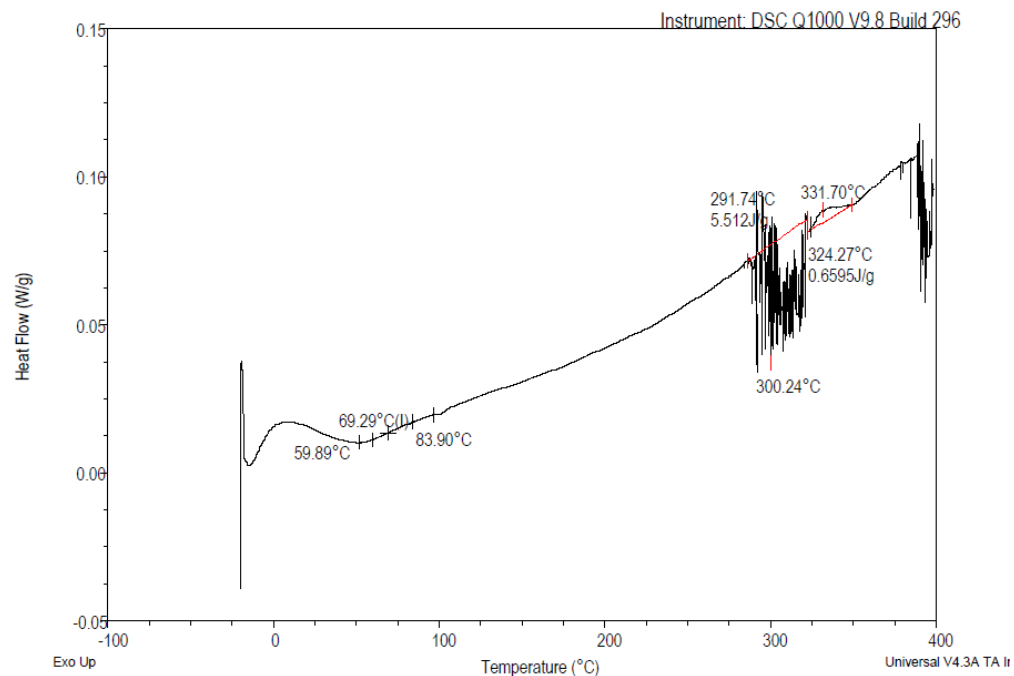


Figure 4.7: DSC of Fernco S301

5.2 Hychem TL5

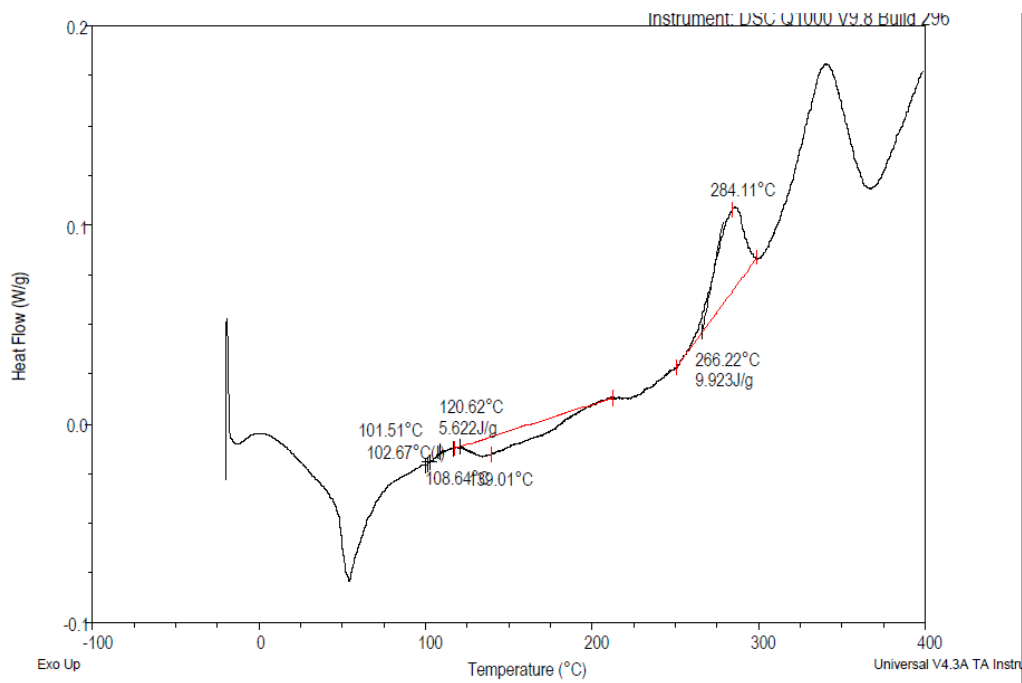


Figure 4.8: DSC of Hychem TL5

5.3 Nitomortar ELS

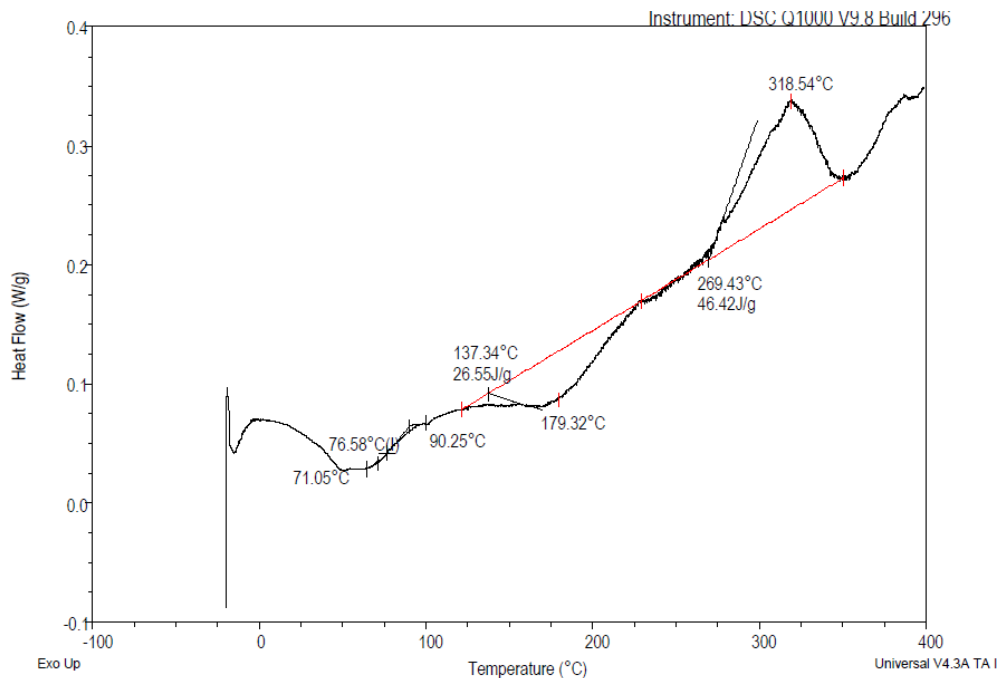


Figure 4.9: DSC of Nitomortar ELS

5.4 Polibrid 705E

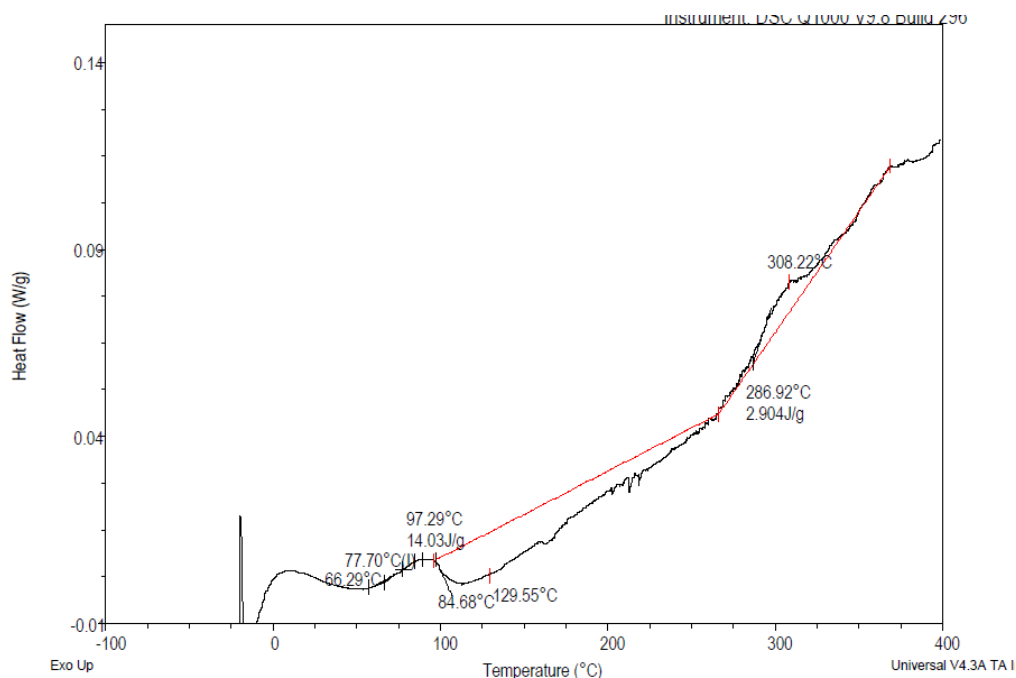


Figure 4.10: DSC of Polibrid

5.5 Sikadur 31

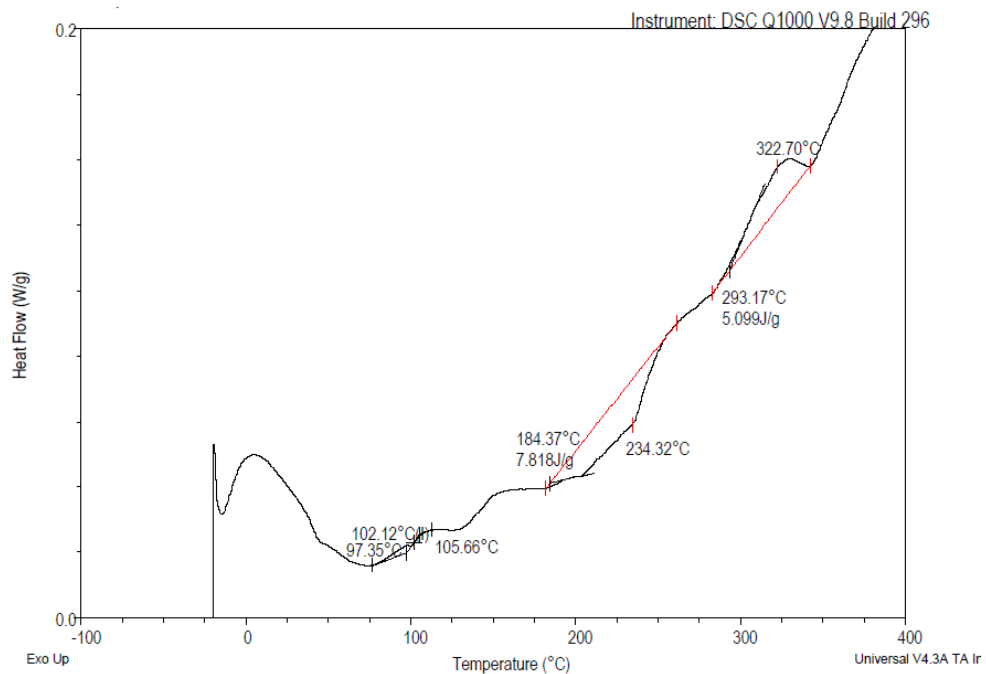


Figure 4.11: DSC of Sikadur 31

5.6 Sikagard 63N

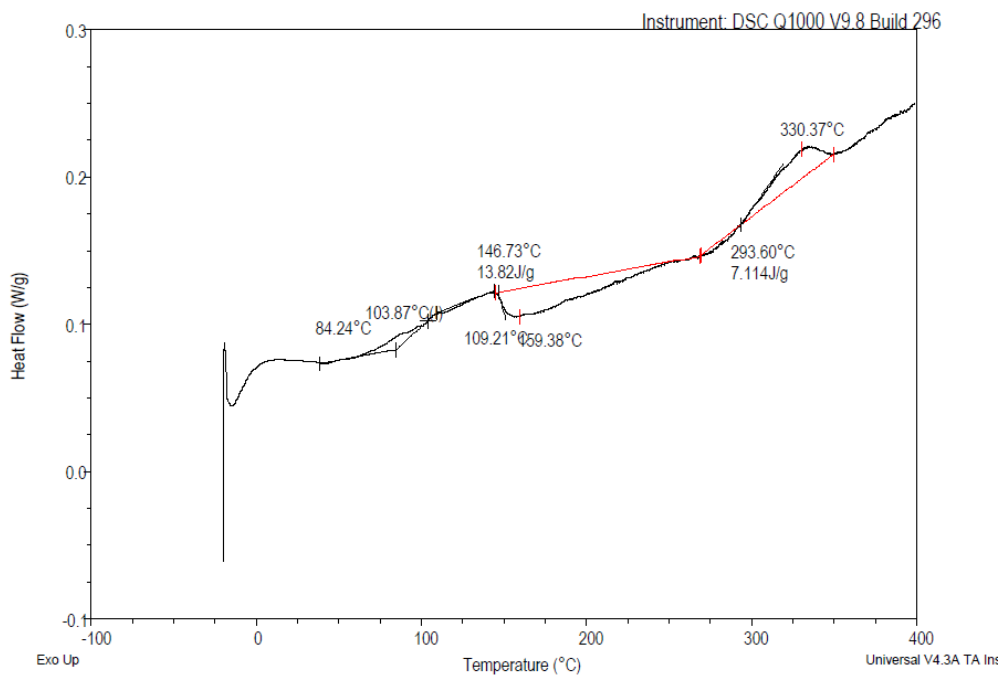


Figure 4.12: DSC of Sikagard 63N

5.7 Sikadur 41

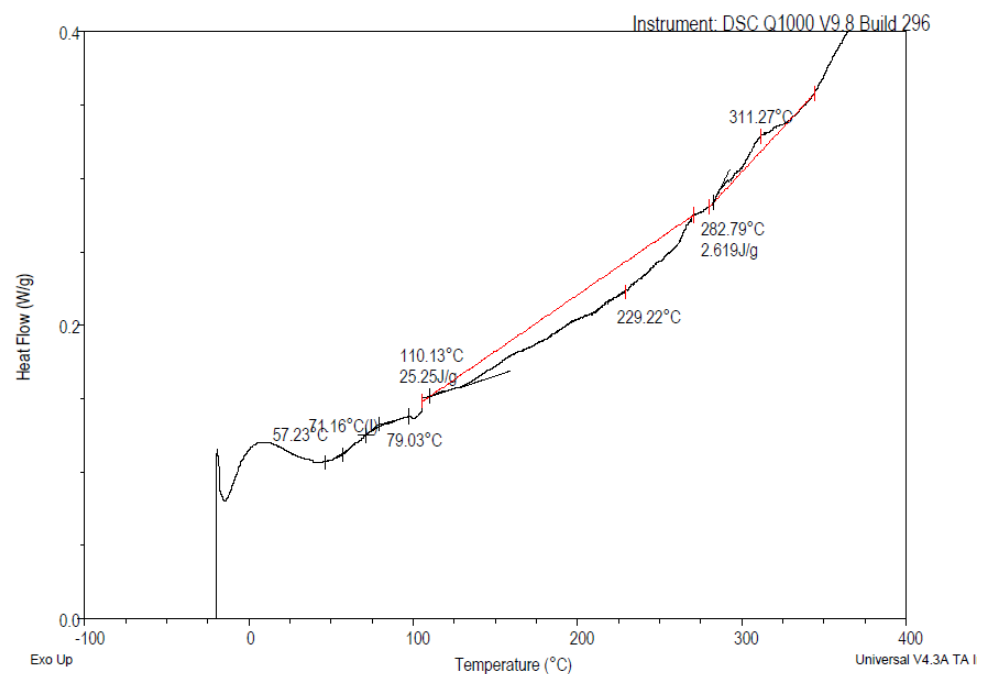


Figure 4.13: DSC of Sikadur 41